

UCLA-ENG-90-05
FY 1989/90
Fall 1989

MECHANO-CALORIC COOLING DEVICE
FINAL REPORT

1989

by

T. H. K. Frederking, Principal Investigator
Jack Luna
P. Abbassi
R. M. Carandang

PREPARED FOR THE
NATIONAL AERONAUTICS AND SPACE ADMINISTRATION
AMES RESEARCH CENTER
MOFFETT FIELD, CA 94035

GRANT NAG-2-516

Department of Chemical Engineering
School of Engineering and Applied Science
University of California, Los Angeles, CA 90024

(NASA-CR-196016) MECHANO-CALORIC COOLING
DEVICE Final Report (California Univ.)
72 0 CSCL 140

NOO-17552

Unclass
63/35 0261068

UCLA-ENG-90-05
FY 1989/90
Fall 1989

MECHANO-CALORIC COOLING DEVICE

FINAL REPORT

1989

by

T. H. K. Frederking, Principal Investigator
Jack Luna
P. Abbassi
R. M. Carandang

PREPARED FOR THE
NATIONAL AERONAUTICS AND SPACE ADMINISTRATION
AMES RESEARCH CENTER
MOFFETT FIELD, CA 94035

GRANT NAG-2-516

Department of Chemical Engineering
School of Engineering and Applied Science
University of California, Los Angeles, CA 90024

TABLE OF CONTENTS

	Page
1. ABSTRACT	1
2. INTRODUCTION	2
3. MACRO-THERMODYNAMICS INCLUDING COOLING COEFFICIENTS	4
4. TERRESTRIAL He I-He II PROCESSING SYSTEMS	12
5. IDEAL μ -P- μ -P CYCLE FOR He II	18
6. SPACE SYSTEMS FOR He I-He II FLUID PROCESSING	27
7. EXPERIMENTS	36
8. CONCLUSIONS	53
APPENDIX A: Abstract of Papers	60
SUPPLEMENT: "1/2 Century of Superfluid He"	65

1. ABSTRACT

The mechano-caloric effect is potentially useful in the He II temperature range. Aside from demonstration work, little quantification effort appears to have been known since other refrigeration possibilities have been available for some time. Successful He II use-related system examples are listed as follows: in space, the utilization of the latent heat of vaporization has been quite successful in vapor-liquid phase separation (VLPS) in conjunction with thermomechanical force application in plugs. In magnet cooling systems, the possibility of using the mechano-caloric cooling effect in conjunction with thermo-mechanical circulation pump schemes, has been assessed (but not quantified yet to the extent desirable). A third example is quoted in conjunction with "superfluid wind tunnel" studies and liquid helium "tow tank" for surface vessels respectively. In all of these (partially future) R&D areas, the question of refrigerator effectiveness using the mechano-caloric effect appears to be relevant, possibly in conjunction with questions of reliability and simplicity. The present work is concerned with quantification of phenomena including simplified thermodynamic cycle calculations.

2. INTRODUCTION

The mechano-caloric effect is a special phenomenon observed in superfluid liquid Helium. (Helium-4 below the lambda point at this time appears to be the liquid of technology interest, and superfluid Helium-3 is not considered.) The effect is the reverse of the thermomechanical effect ("fountain effect"). A difference in temperature (T), applied to He II in a special device such as a porous plug, produces a difference in pressure (P). The latter is called thermomechanical pressure difference. The ideal case is described by the London equation, for constant chemical potential (μ), as

$$(\partial P / \partial T)_{\mu} = \rho S \tag{2.1}$$

(ρ liquid density, S entropy per unit mass). There have been sufficient laboratory applications

stimulating use in space for transfer from a supply vessel to a receiver vessel. The reverse effect, the mechano-caloric effect, is described by

$$(\partial T / \partial P)_{\mu} = 1 / (\rho S) \quad (2.2)$$

A pressure reduction from P to $(P-dP)$ causes a temperature reduction noting that the density and entropy have to be positive in matter which is stable. In relation to Eq. (2.2), little work has become known, possibly because of an initial emphasis on obtaining devices which produce low temperatures conveniently. Less emphasis has been on high effectiveness expressed most often in "coefficient of performance" (COP) numbers in refrigeration cycles. An early outstanding mechano-caloric effect utilization example has been the "vortex refrigerator" of Staas and Severijns (1969). Vortices generated from superfluid are involved in various components of the systems, and keeping track of the vortex motion, Staas et al. have been able to describe the performance of the refrigerator in "vortex language" terms. It appears to be desirable to supplement their work using continuum tools, such as thermodynamic cycle analysis. This is one part of the present studies which attempt to summarize highlights of preceding work. In this introduction additional comments are made on various schemes providing cooling in the He I (above the lambda point)/He II range, often relying on the use of the latent heat of vaporization.

Claudet, Bon Mardion, Seyfert and Verdier et al. (1974-1980) have been instrumental in the development of a JT (Joule-Thomson) subsystem which supplies cooling for a pressurized He II bath underneath a He I bath (usually at atmospheric pressure). (Pressurized He II is designated as He II_p, saturated He II as He II_{sat}.) Latent heat of vaporization, used in the auxiliary JT loop, has to "lock in" unto the "binodal" (vapor-liquid equilibrium curve) in the He II range. Thus, a pump is necessary. For magnet test facilities with large liquid volumes, long cooldown times are required for a specified pump with limited capacity. A different version of this He II-He I "hybrid system" has been reported by Hosoyama et al. (1982). Another system of the same "family" has been described by Hakuraku (1983). Recently, Sato (1989) has outlined a magnet

cooling system with a rather short cooldown time using only a small liquid volume and indirect cooling. While these systems avoid pumpdown, it is remarked that the Elsner-Klippping system (1969) for terrestrial He II bath replenishment permits another type of liquid transfer. Further, adiabatic demagnetization techniques are potentially useful in conjunction with available superconducting magnets in the 10 Tesla range. There appear to be interesting alternate routes as soon as "high- T_c " superconducting metal oxides have become viable technology materials for refrigeration purposes. Aside from all of these systems, using condensed matter as superconductors and/or superfluid liquid, there has been the demonstration of multi-stage pumps (Severijns, 1980) with the purpose of circulating liquid He^4 in a Helium-3/Helium-4 dilution refrigerator.

A special aspect of superfluid wind tunnels/tow tank facilities (Donnelly et al., 1989*) is the observation that the smallest liquid shear viscosity has been found as *normal* fluid shear viscosity in He II near 1.7 K. (The two-fluid model assigns a finite shear viscosity to the normal fluid component.) According to the two-fluid model, there are two components, the superfluid and the normal fluid. An interesting property is the character of the normal fluid: it appears to be some sort of a special Newtonian fluid (while superfluid, to some extent, has Euler fluid properties). Thus, as long as continuum conditions prevail, there appears to be a chance to model bodies in the low shear viscosity system available as He II (noting the restrictions imposed on such a system). An example is the aerodynamics and aero-acoustics of the fast moving levitated train. For instance, for the "Mag-Lev" (magnetic levitation) travel scenario of future transportation systems, 500 km/hr (300 miles/hour) have been envisioned. The conventional train at 250 km/hr reaches about 80-90 dB, and relatively unknown noise levels at 500 km/hr appear to generate much interest in further noise reduction. Using a cross section on the order of 10 m^2 , a vehicle length on the order of 10 m, a speed of 500 km/hr, or about 140 m/s, in conjunction with a kinematic viscosity of air on the order of $15 \times 10^{-6}\text{ m}^2/\text{s}$, we have an order of magnitude of the Reynolds number of 10^8 . Using the kinematic viscosity of He II, for a speed on the order of 2

*Abstracts of the 92nd Annual Fluid Dynamics Conf., November 1989.

m/s with a model length scale 0.5 m/10 m (= 1:20), one arrives at the same order of the Reynolds number. The dissipation, for a model vehicle with a cross section on the order of 0.025 m^2 , is based on a drag coefficient order of magnitude 0.1. The related force reaches the order of 1 Newton. The power dissipation, due to aerodynamic drag, has the order of 1 Watt. This order of magnitude example suggests that the refrigeration system choice for continuous "superfluid wind tunnel" operation appears to be an interesting question. It is noted that quite a few forced convection studies in He II have led to "classical fluid flow conditions noting, however, that the drag crisis, e.g., on a sphere, has not been quantified to the extent desirable.

After these introductory remarks, the present report considers the sections listed in the "Table of Contents" along with supplementary information.

3. MACRO-THERMODYNAMICS INCLUDING COOLING COEFFICIENTS

Macroscopic thermodynamic changes of state of continuous media are considered. First, thermodynamic cycle quantification based on suitable performance measures is discussed. Second, various derivatives are described which may be useful in the context of refrigeration cycles involving He I/He II fluid states.

The characterization of the quality of a single-component refrigeration cycle is quite often based on *ideal* reference cycles. "Effectiveness" values, "efficiency" and/or "figures of merit" may be defined in relation to the ideal cycle. The latter, in turn, may be limited by constraints on the cooling coefficient. Extensions to multi-component cycles have been known for some time. One advantage in this area of chemical thermodynamics applications may be the use of "waste heat" powering the process.

In mechanical vapor compression systems, the input is mechanical pumping power (fluid compression power). The desired effect in refrigeration is the refrigeration load handled per unit time. Referring to the power (\dot{W}) per mass flow (\dot{m}) unit (= work per unit mass), we consider the

ratio of the refrigeration load (\dot{Q}_c) to the input work ($\dot{W}/\dot{m} = \dot{W}$). This ratio is defined as coefficient of performance (COP) of the cycle:

$$\text{COP} = Q_c/W \quad (3.1)$$

The chemical thermodynamics process takes in heat at a temperature $[T > T_e]$ above the room temperature (environmental temperature T_c). In some cases space heating is desired, and this quantity is the desired effect to be related to the input heat. In the present context of refrigeration, however, the following definition is suitable:

$$(\text{COP})_{\text{ch}} = Q_c/Q_H \quad (3.2)$$

Pump efficiency comparison. In He II-He I systems under consideration, the question frequently coming up in recent years is as follows: is the mechanical pump superior in "efficiency" compared to the thermomechanical pump using the He II thermomechanical effect? This question is not quite fair and appropriate for a full assessment as the thermomechanical pump responds to *heat input*. If sufficient "waste heat" is available, the mechanical pump cannot "compete" in this area as it is incapable of using input heat *directly*. Examples of heat inputs are imperfect insulation systems or special heat input components.

The comparison immediately suggests a similarity of the He II behavior to chemical thermodynamics cycles as far as "heat" utilization goes. It is noted that the simple heat representation in the entropy-temperature $[T-S]$ diagram as "area-under-a-curve" does not apply in general. Important "cold" energies and heat contributions are $T \times S$ terms in He II. Thus some caution is needed when "classical" thermodynamics methods known from vapor compression cycles are extended to quantify He II cyclic operation.

Turning to cooling coefficients as important constraints, we may consider the definition $\alpha_j = (\partial T / \partial P)_j$ at constant thermodynamic quantity "j". Examples are constant enthalpy ($dH = 0$), constant entropy ($dS = 0$), constant chemical potential ($d\mu = 0$) and others.

JT-system cooling constraints $(\partial T/\partial P)_H$. This coefficient (derivative) has been important in the Joule-Thomson Linde Hampson type cryocoolers and plants. Using the isobaric expansion coefficient $\beta = (\partial \ln v/\partial T)_P$ we write

$$(\partial T/\partial P)_H = 1/(\rho c_p) \cdot [\beta T - 1] \quad (3.3)$$

(v = specific volume = $1/\rho$; ρ density; c_p specific heat at constant pressure). For the weakly imperfect gas, the van der Waals fluid model permits a useful (qualitative) insight: the result for $(P + a/v^2)(v - b) = RT$ (1 mol; v volume = $1/\rho$; R universal gas constant at 8.314 J/(mol K); a, b van der Waals coefficients) at low pressure is written using normalization in terms of critical quantities (subscript c). One may express the attraction parameter as

$$a = (27/64)(RT_c)^2/P_c \quad (3.5)$$

Further, the repulsion parameter is

$$b = (1/8)RT_c/P_c \quad (3.6)$$

The cooling coefficient is rewritten in terms of the second virial coefficient $B(T)$. The resulting equation is

$$\alpha_H = (T/c_p)[dB/dT - B/T] \quad (3.7)$$

The low- P version of van der Waals' equation involves a second virial coefficient of

$$B(T) \approx b - a/(RT) \quad (3.8)$$

Thus, the low pressure cooling coefficient becomes

$$\alpha_H = (1/c_p)[(2a)/(RT) - b] \quad (3.9)$$

Therefore, the *maximum inversion temperature* ($T_{i,max}$) is available ($\alpha_H = 0$) as approximate value of the ratio ($T_{i,max}/T_c = 2a/RTb$). Insertion of a and b leads to

$$T_{i,max} = (27/4)T_c \quad (3.10)$$

It turns out that cooling has to be accomplished by other means above the maximum temperature

of the inversion curve. However, the ratio ($T_{i,max}/T_c$) for low temperature fluids (Helium-3, Helium-4, hydrogen isotopes, neon) is lower than the value (27/4) of the result (3.10). The inversion curve in the Helium-4 P-T phase diagram hits the "binodal" (vapor-liquid equilibrium curve) at about 4.5 K (McCarty Tables, 1977). Another interesting feature of He I near the lambda point is the existence of the maximum in density with $\beta = 0$. It turns out that any convection at this point, according to a simple shock model (Caspi et al., 1986) leads to a Mach number of first (ordinary) sound of unity. Below this maximum, i.e. in a domain very close to the lambda temperature (T_λ) the calculations suggest existence of a "shock layer". The layer is similar to other shock domains insofar as it appears to be very thin. It is supportive of a well-defined interfacial domain for coexisting He I and He II. This coexistence involves transport. It is noted that the model is based on the assumption of *local* thermodynamic equilibrium.

In the He II range, the JT coefficient, or cooling coefficient $(\partial T/\partial P)_H$ reaches negative values as long as β is negative. This implies *heating* upon imposition of the pressure reduction in the throttling process. The specific heat per unit volume, $c_p\rho$, however, is quite small. Therefore, the T increase becomes small. Moreover, the thermomechanics/mechanocalorics of He II appears to be dominant as long as the entropy is large. In this context, Huang (1986) has pointed out that at low T, where S is very small, the JT cooling coefficient becomes significant again as soon as T has dropped far enough below T_λ . For details the tables of Huang (op cit.) may be consulted.

In the use of JT systems for cryocoolers, the initial system startup has to rely on a state below the maximum inversion temperature. As soon as the system has reached a low temperature, the major impact comes from the throttling into the two-phase regime with vapor-liquid coexistence. The common terminology of the liquid production includes the liquid yield ($y = 1 - x$; x "quality" = vapor mass fraction per total two-phase mass). The isenthalpic throttling process may be characterized by an equality in upstream (H_u) and downstream enthalpy (H_d), or

$$H_u = yH_L + (1-y)H_v = H_d \quad (3.9)$$

From this ideal change of state the liquid yield is obtained as

$$y = (H_v - H_u)/(H_v - H_L) = (H_v - H_u)/\lambda \quad (3.10)$$

(H_L saturated liquid enthalpy, H_v saturated vapor enthalpy, λ latent heat of vaporization). Figure 3.1 is a schematic plot of the pressure-temperature diagram with arrows indicating qualitatively the direction of the state change for throttling ($dP < 0$).

Isentropic coefficient $(\partial T/\partial P)_s$. The use of isentropic changes of state, via external work removal in an expansion process, has been most effective if the expander has a high efficiency. The cooling coefficient is

$$\alpha_s = (\partial T/\partial P)_s = \beta T/(\rho c_p) \quad (3.11)$$

Ideal gas is characterized by $(\beta T) = 1$. Further, the mass-related difference between c_p and c_v , the specific heat per unit volume, is $R_i = c_p - c_v$ (R_i individual gas constant R/M_i ; M_i molecular mass of substance i). The equation of state is written in terms of these quantities as $\rho = P/(R_i T)$. Insertion of these constraints into (3.11) leads to the result

$$(\partial T/\partial P)_s = [P/T](\gamma - 1)/\gamma \quad (3.12)$$

(γ = specific heat ratio c_p/c_v). The largest values of the specific heat ratio occur in monatomic gas (in ideal gas states), e.g. Helium. Ideal gas conditions, however, are left behind as the fluid becomes dense at low T . The density grows up to the density maximum located a few milli-K above T_λ . At the density maximum ($T = T^*$) we have $\beta = 0$, thus α_s becomes zero. There is no change in T as the pressure changes from P to $(P - dP)$. For the temperature range $T_\lambda < T < T^*$, the expansion coefficient becomes negative. Therefore, the temperature *increases* upon an infinitesimal *decrease* in pressure.

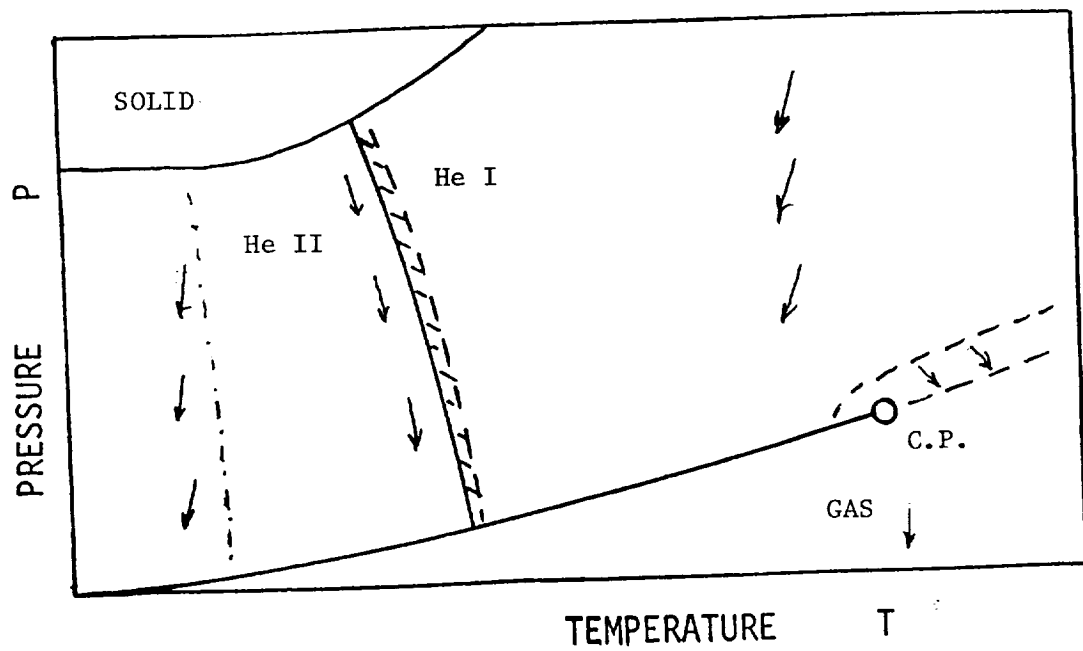


Fig. 3.1. Pressure (P) - Temperature (T) phase diagram for He^4 , schematically;
 // "shock domain" with Fourier heat conduction due to "thermohydrodynamic shock" ;
 Arrows indicate direction of T-change upon throttling $dP < 0$;
 C.P. critical point
 -.- line with zero isobaric expansion coefficient.

Special conditions at the lambda point are discussed using the Grueneisen parameter $\Gamma_G = \beta/(\rho c_v K_T)$; K_T isothermal compressibility - $(\partial \ln v/\partial P)_T$. The isobaric expansion coefficient may be expressed as

$$\beta = \rho c_v K_T T_G \quad (3.13)$$

The isentropic coefficient is rewritten as

$$(\partial T/\partial P)_s = \beta T/(\rho c_p) = (c_v/c_p) K_T \Gamma_G T \quad (3.14)$$

There are weak anomalies of lambda-shaped quantities. Examples are K_T , Γ_G and c_v while c_p is distinctly lambda shaped. Therefore, no strong enhancement of $(\partial T/\partial P)_s$ may be expected at the lambda transition. The peculiar effect of *cooling*, upon work supply in a pump, is predicted for He II. However, its magnitude is quite small, and, depending on the scale of the P-T diagram used, the decrease may look nearly like an isotherm. No verification of the cooling effect appears to have been reported yet. In fact, He II pump operation observed has shown T increases due to irreversibilities.

In He II there is a *negative* isentropic cooling coefficient until the density minimum is reached. *Below* the temperature of the density minimum, we have again $dT < 0$ for $dP < 0$.

The conditions are displayed schematically in the P-T diagram (Fig. 3.2). As ideal isentropic changes of state are reversible, the arrows may point in both P directions, i.e. $dP < 0$ and $dP > 0$.

Isochoric cooling coefficient $(dT/dP)_v$. The constant volume change is the *ideal* reference state change in regenerator-based small cryocoolers. The derivative under consideration is the reciprocal "pressure coefficient". The cooling coefficient is expressed as

$$(\partial T/\partial P)_v = K_T \beta = 1/[\Gamma_G \rho c_v] \quad (3.15)$$

There is a sign reversal when β changes sign. This behavior is quite similar to the isentropic

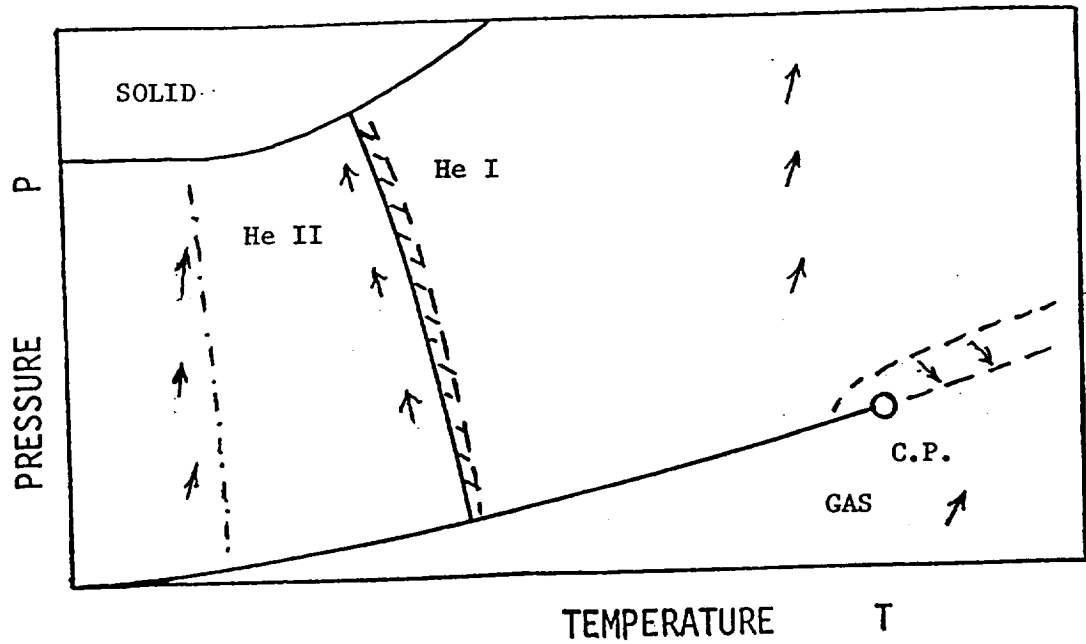


Fig. 3.2. Pressure - temperature phase diagram of Helium-4,
schematically; C.P. thermodynamic critical point ;
Arrows indicate direction of T-change during compression;
 $dP > 0$;
-.- zero isobaric expansion coefficient at density minimum,
schematically ;

case. It is noted that regenerators need a large heat capacity for useful operation of a cooling cycle.

Constant chemical potential coefficient $(\partial T/\partial P)_\mu$. The effect is restricted to superfluid liquid. Again reversible conditions prevail in the limit of zero irreversibilities.

For pumping ($dP > 0$), by means of $dT > 0$, useful operation has to keep the important pump component below T_λ while restricted liquid domains may reach into the He I range. The "pump diagram" $P(T)$, with constant chemical potential curves included, may give a first idea about the ideal thermostatics of various state changes ($dP = \rho SdT$).

Cooling might be read from the $P(T, \mu)$ diagram as soon as upstream and downstream pressures have been specified. The cooling coefficient is

$$\alpha_\mu = (\partial T/\partial P)_\mu = 1/(\rho S) \quad (3.16)$$

The entropy is a strong function of T , while the liquid density is a very weak function of T . Thus, at low T , the cooling coefficient is large. The use of porous plugs as mechano-caloric components has to avoid axial heat conduction as far as possible. Eventually, axial heat leaks compensate for the cooling effect, and the *ultimate* temperature is reached (Hendricks, 1989). For cyclic operation, the performance is important as well. Therefore, it is mentioned briefly that ideal cycles (Section 5) suggest favorable COP values for temperatures near the lambda point.

4. TERRESTRIAL He I- He II PROCESSING SYSTEMS

Liquid processing phenomenology. By the end of the 1960's basic phenomena of fluid flow through porous media components started to get on the agenda of various research and development teams. The quest for quantification of various phenomena apparently had become more urgent. This action had been based on the 1937-1939 superfluidity discoveries which

demonstrated the crucial role of the narrow channel devices. A vivid account of that early "pioneer period" of time has been given by Professor Jack Allen at the CEC/ICMC'89 (paper GC-O1). Other speakers of that session have contributed various subsequent findings and developments of concepts in the superfluid He II area.

Concerning a classification of possible phenomena the papers of DeLong-Symco-Wheatley (1971), Klipping et al. (e.g. Elsner-Klipping 1969 and 1973), Kreitman (1969, 1971) and others showed a variety of flow implementation schemes. Another area of great activity has been the exploration and utilization of He II-He I coexistence. Starting with Roubeau's observation (Roubeau 1971) and utilization, as described by Biltcliffe, Roubeau et al. (1972), "lambda systems" have been developed. "Light" He I is kept above "heavy" He II near the lambda point.

The next phase in the development of pressurized He I baths above He II has been conducted by the group in Grenoble : Claudet, Lacaze, Roubeau, Verdier (1974) and Bon Mardion-Seyfert- Vallier et al. have been contributors. Without subtracting from these very interesting contributions of the group collaborators, the systems are referred to as Claudet et al. systems. (Apologies are due for using this simplified nomenclature which does not mention the individuals pioneering in the field explicitly.) After these introductory remarks on the terrestrial systems, several aspects are taken up. It is noted that the terrestrial systems have been aimed quite often in the direction of magnet test facilities. However, several developments consider space cryogenics scenarios (to be discussed in section 6). Again, the following characterization of fluid states is used:

He II_p, pressurized superfluid He II;

He II_{sat}, saturated liquid He II.

Similar subscripts are applicable in the He I case noting however that the liquid behavior may be quite "classical" lacking the thermomechanics of He II.

An example of the liquefaction conditions for $\text{He II}_{\text{sat}}$ production is given in Fig. 4.1. Throttling is ideal isenthalpic pressure reduction to the 1.8 K bath. The starting points involve bath temperatures in the He I range. Steady flow is presumed. This implies that heat input into He II will vaporize liquid such that replenishment is needed. Also, the He I bath on the top has to be kept at constant liquid level. Figure 4.2 shows that y_{JT} is above 0.8 near 2.5 K, however when 4 K is approached the yield drops below 0.7.

The T-S diagram for the entire (ideal) process is shown in Fig. 4.2. The idealized process assumes cooling from point 1 to point 2 on an isobar. (The isobar is close to the saturation line.) Throttling takes place from point 2 to point 3. At point 3 two-phase conditions cause separation of saturated liquid (L) from saturated vapor (V). Finally, warmup occurs from point (v) ideally to point 4.

Figure 4.3 is a schematic diagram of the modified "Claudet et al. system". $\text{He II}_{\text{sat}}$ is produced in an auxiliary bath. The latter is coupled via a heat exchanger to the He II_p bath underneath the He I at 1 atm. The actual conditions in the He I bath are characterized by T-gradients since He I has a small thermal conductivity. It is convenient to extract He I at the coldest spot of the upper bath. This leads to the highest liquid yield. An example of this nature has been given by Castaing et al. (1987).

Essential points are summarized as follows: the auxiliary bath of saturated $\text{He II}_{\text{sat}}$ requires pumping capability which may require a substantial vacuum pump capacity; the use of a beneficial temperature gradient in the He I domain may reduce the heat exchange surface needed for operation in He II near the lambda point. In space, there is sufficient "vacuum pumping" available; however, the latent heat of vaporization used in the modified Claudet et al. process makes this system a "passive device" such that helium is lost to the surroundings.

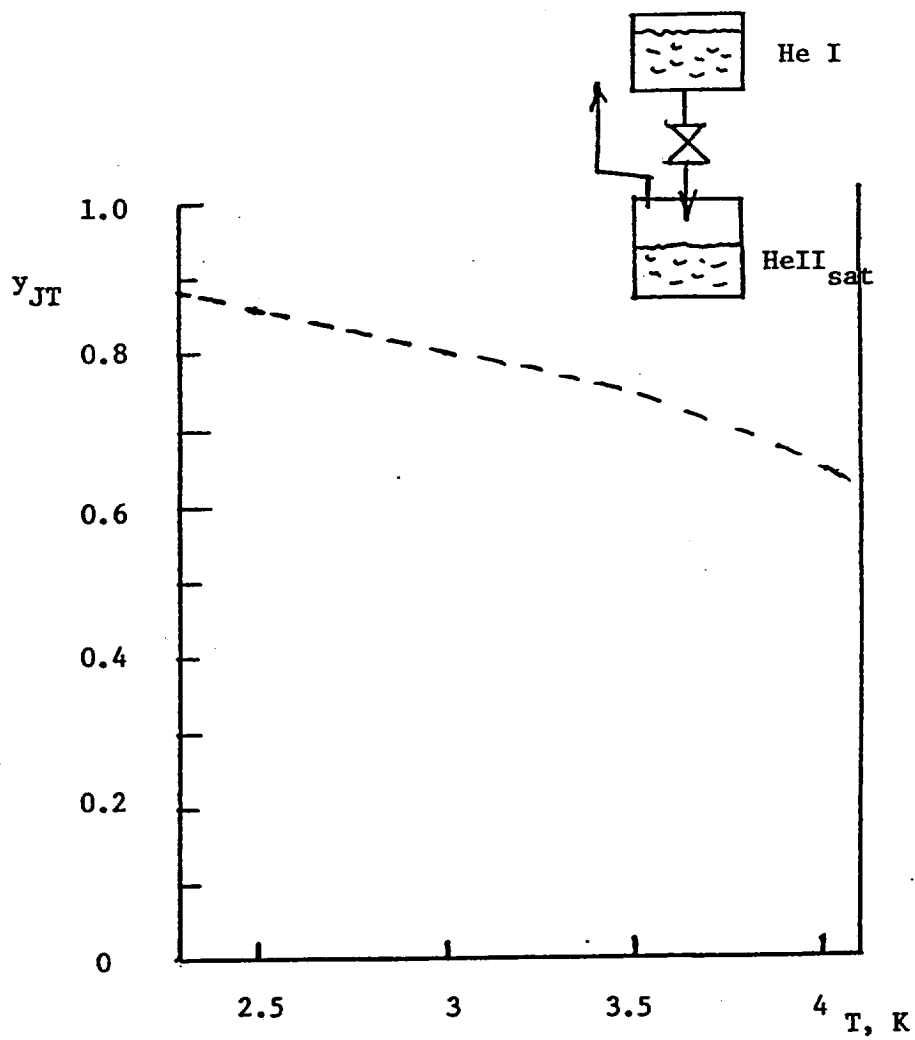


Fig. 4.1. Example of throttling of He I to liquid He II at 1.8 K : liquid yield y_{JT} as a function of the initial bath temperature ;
Assumption : ideal, quasi-steady process.

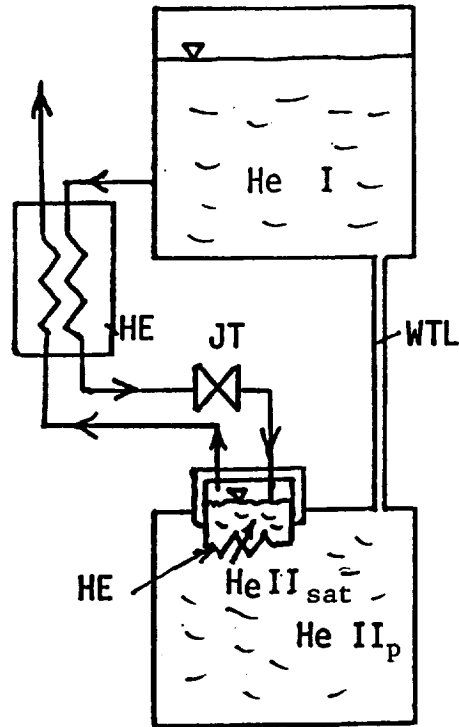


Fig. 4.3. Modified "Claudet et al system" for processing of fluid in the auxiliary JT system for the dual bath He I_{sat} (1 atm) and He II ; HE heat exchanger ; JT throttling valve ; WTL "weak^p thermal link" = thermal component providing He II_p and He I_p coexistence.
(From Carandang et al. ,1986).

He I : upper domain is close to He I_{sat} (1 atm);
lower domain is subcooled.

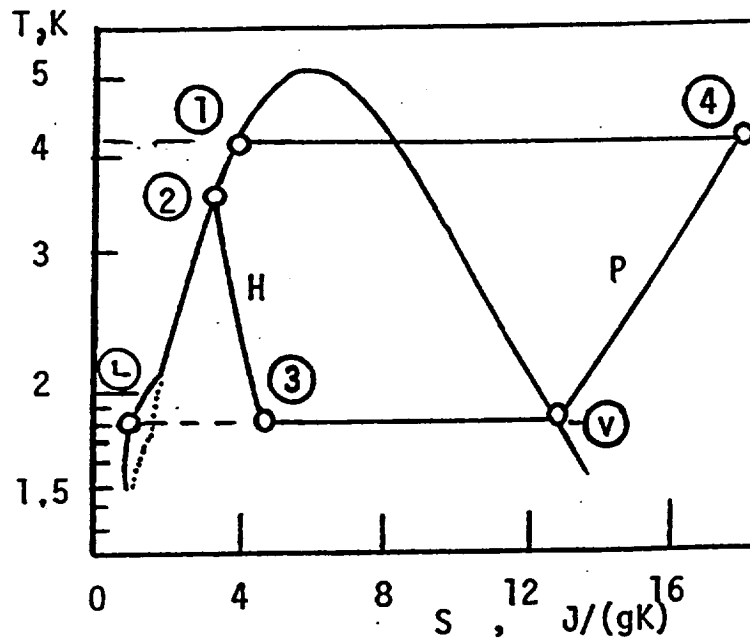


Fig. 4.2 . Schematic graph of cycle sequence (ideal case)
of modified Claudet et al processing system in the
temperature -entropy diagram (log T-vs S);
Cycle : 1-2-3-4-1 ; (or P-H-P-T);
1-2 ISOBAR; 2-3 ISENTHALPIC CURCE; 3-L ; (L saturated
liquid ; 3-v ; 3-v saturated vapor ;
L-4 ISOBAR ; 4-1 ISOTHERM .

5. IDEAL μ -P- μ -P CYCLE FOR HELIUM II (SUPERFLUID HELIUM-4)

The cycle consists of isobaric changes ($dP = 0$) and of iso-potential changes (chemical potential increment $d\mu = 0$). In general it is noted that there has been a relatively small number of reports on cyclic operation involving either thermomechanical pressure increase, or mechano-caloric changes of state, or both. The ideal cycle, considered in the present section 4, appears to be among the simple possible choices of ideal state change sequences.

The question coming up in this area may be formulated as follows: why do we have only a limited knowledge of cycle applications in the He II area? A (partial) answer seems to be related to the fact that in the T-range from 1 to 2 Kelvin there are sufficient cooling techniques available which alleviate the need for alternate systems.

Nevertheless it is noted that there are the various "Claudet et al." refrigerators, and variations thereof reported by Warren et al. (1980), Hosoyama et al. (1982), Hakuraku-Ogata (1983), Sato (1989) and others.

The first demonstration of He II cooling without moving components appears to be the Staas-Severijns He II "vortex refrigerator" (Staas-Severijns 1969).

Cooling limitations in this area have been discussed by Hendricks (1989). Other work has pointed out the advantage of a high coefficient of performance predicted for ideal systems (Frederking et al. 1988). Alterations in the direction of multi-stage fountain effect pump systems are demonstrated in the system of Severijns (1980). Obviously several state change combinations, and cycle variations appear to be possible in this relatively restricted temperature range. Therefore, a few features will be discussed briefly.

The option of a *power* system demonstration may be raised. However, this cycle direction is rather unattractive as the density (volume) changes of the working fluid are rather small.

(A model exception for small loads is the spider demonstrated by Kapitza, e.g. Atkins 1959.) The small volume changes induce questions for realistic performance data as this type of fluid appears to make *refrigeration* an attractive option. A special condition is the negative expansion coefficient of He II in the T-range between the lambda temperature and about 1.2 K. This property is reminiscent of water between 273 K and 277 K. In contrast to water, the thermomechanics is accompanied by heat evolution more in line with chemical thermodynamics than with single-component behavior.

A brief inspection of the refrigeration/cryocooler literature reveals a nearly complete lack of He II vortex cooler listings. Therefore, two essential components are considered first in a qualitative sense (Fig. 5.1). The pressure increase in the FEP unit has been the topic of a lot of recent interest in liquid He II transfer in space (section 6). The Staas-Severijns system demonstration fortunately has included both, the use of a mechanical (centrifugal) pump and the use of a stationary FEP. This experience with both types of pressurization systems induces confidence concerning "mechano-caloric depressurization". Rather little knowledge, outside qualitative experimental findings in ideal geometries, appears to be available on this point. Yet, the data base on other components of the cycle has provided a lot of insight. Thus, the method of induction arguments may be used for the unknown features of the mechano-caloric component along with the Staas-Severijns findings.

Ideal reference cycle. The ideal sequence involves abrupt changes of state at points 2 and 4 (Fig. 5.1) where several constraints are imposed. In detail we have the sequence (Fig. 5.2) 1-2-3-4-1 with

- 1-2 constant chemical potential P-increase;
- 2-3 aftercooler, ideally at $dP = 0$ back to the initial temperature, i.e. $T = T_i$;
- 3-4 iso-potential depressurization with $dP < 0$ $dT < 0$, i.e. mechano-caloric cooling;

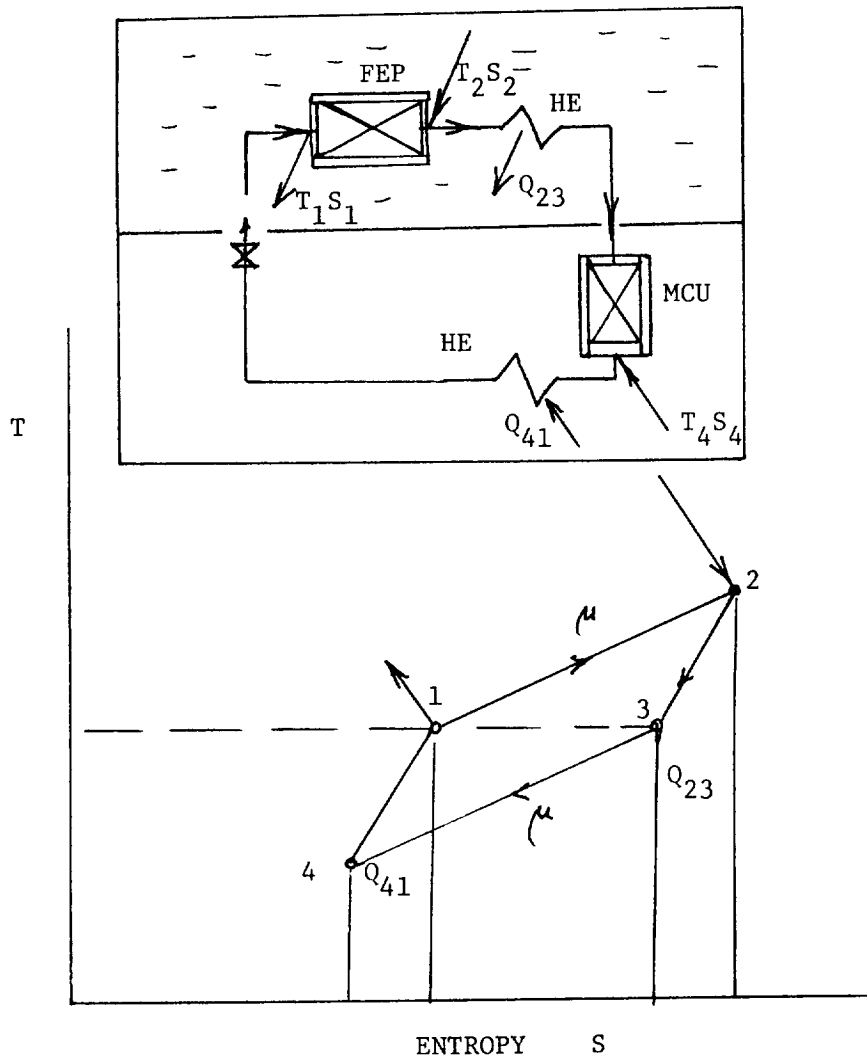


Fig. 5.1. Idealized vortex refrigerator cycle μ -P- μ -P;
T-S diagram , schematically ;

Inset : FEP fountain effect pump (TM pump=thermomech.pump);
HE heat exchanger
MCU mechano-caloric unit

4-1 heat supply, ideally at $dP = 0$.

The last state change departs from the design of the Staas-Severijn system. The latter has an adiabatic component after point 4, i.e. the real (non-ideal) point 4. Thus, vortex shedding processes and their effects on the cycle have been accessible in the early pioneer work of these authors.

A peculiar aspect is the "chemical thermodynamics" feature of the process with heat evolution. This may be understood as an outcome of the two-fluid model with normal fluid, the entropy carrier fluid, and superfluid lacking entropy. The heats evolving at points 1 and 4 are TS terms. The heat exchanger isobars contain "classical" thermal energies "seen" as areas-under-a-curve in the T-S diagram. In order to avoid confusion of overlapping areas in a T-S plot, we make use of arrows representing (TS) heat evolution terms (Fig. 5.1).

Figure 5.1 is distorted somewhat for purposes of illustration. Individual state changes are discussed subsequently.

State change. The isopotential change from 1 to 2 is idealized using the notion of an ideal superleak (ISL). There are only thermostatic changes with a pressure rise according to the London equation. Kinetic energy effects are neglected.

$$\Delta P_\mu = P_2 - P_1 = \int_{T_1}^{T_2} \rho S(T) dT \quad (5.1)$$

The pressure influence on the entropy is relatively weak. Also the density variation is rather weak. Therefore, a first order approximation is

$$\Delta P_\mu \approx \rho \int_{T_1}^{T_2} S(T) dT \quad (5.2)$$

The heat evolution is a result of two-fluid properties: only superfluid can pass through the ISL. The very narrow fluid passages of the ISL immobilize the normal fluid because of its finite shear viscosity. Superfluid flow tends to increase the "concentration" of superfluid at the warm

(downstream) location. Heat input at the rate $\dot{m}T_2S_2$ prevents the system from cooling down (\dot{m} mass flow rate, subscript d and u denote downstream and upstream location respectively).

On the upstream side the two-fluid properties tend to increase the normal fluid concentration as fluid leaves. This is to be prevented by entropy and heat removal. For the mass flow rate \dot{m} , the thermal energy removal rate is $(\dot{m}T_1S_1)$. The heats $Q_1 = T_1S_1$ and $Q_2 = T_2S_2$ are indicated in the T-S diagram by arrows noting that T S are rectangular areas.

The isobaric T-reduction in the aftercooling process from 2 to 3 is represented as "classical" area-under-a-curve" in the T-S diagram. The heat removal rate is

$$\dot{Q}_p = \dot{m} \int_{T_2}^{T_3} c_p dT \quad (5.3)$$

($T_3 = T_1$). The subsequent change from 3-4 at $d\mu = 0$, and the isobaric change from 4 to 1 is treated in the manner used for the first part of the cycle.

Performance figures for the process may be adopted from the point of view of an "environmental temperature" (T) in the He II range. For the Staas-Severijns system the heat T S is the useful (ideal) refrigerator load. Therefore, the COP for this system is defined as (Fig.5.2)

$$\text{COP}_{\text{st-s}} = Q_4/Q_2 = T_4S_4/(T_2S_2) \quad (5.5)$$

For the possibility of using the isobaric heat $Q_{41} = Q_p/Q_{41} = Q_p$ the following ideal COP may be defined

$$\begin{aligned} \text{COP}_i &= (Q_4 + Q_{41})/Q_2 \\ &= [T_4S_4 + \int c_p dT]/(T_2S_2) \end{aligned} \quad (5.5)$$

Cycle improvements. Among the possibilities are multi-stage pumps, e.g. 4-stage pump of Severijns (1980), 2-stage pump, Kittel (1988). The multi-stage pumping system may be complemented by iso-potential multi-stage "expansions".

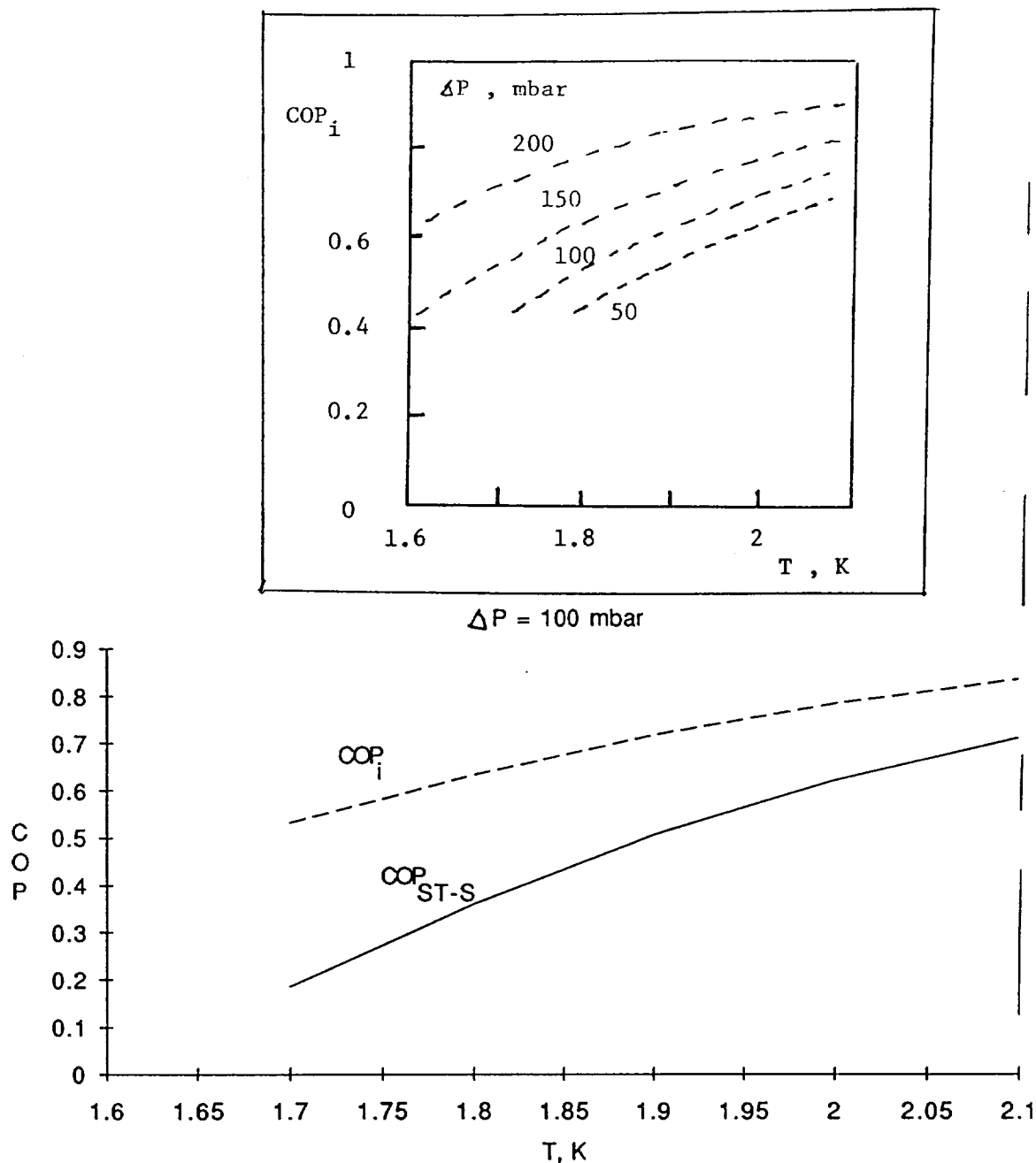


Fig. 5.2 . Coefficient of performance (COP) for the vortex refrigerator ;
 COP_i ideal COP values; COP_{ST-S} Staas-Severijns system;
Inset: COP_i for various pressure increases;
 Abscissa : Bath temperature T_1

Literature on the pressure rise (point 1 to point 2 ,Fig.5.1) has been quoted in the subsequent Table 5.1 on FEP or TM pump papers . Literature on transfer systems has been listed in Table 5.2 as general transfer topics . Literature on mechanical pumping devices is listed in Table 5.3.

Table 5.1. Authors of papers on FEP (Fountain Effect
Pump) systems ;(or TM =thermomechanical pumps)

Arp 1986
 Broulik-Hess 1978
 Elsner 1973 ; Elsner-Klipping 1969,1973

DiPirro 1989
 DiPirro-Boyle 1988
 DiPirro-Castles 1986
 DiPirro-Kittel 1988

Frank-Yuan 1988
 Frederking et al. 1988
 Frederking-Kittel-Nast-Liu 1986

Green 1989
 Hermanson- Mord-Snyder 1986
 Hofmann and Hofmann et al. 1986
 Kittel 1985
 1986 , 1988

Mord et al. 1986
 Nast et al. 1986
 Schmidtchen-Denner 1987
 Severijns 1980

Srinivasan-Hofmann 1985
 Staas - Severijns 1969
 Yuan Frank 1988
 Yuan-Nast 1987

Table 5.2 Authors of papers on transfer line
phenomenology and related work

Anderson 1989
Arp 1986
Brooks 1986

DiPirro-Castles 1986
DiPirro-Kittel 1988
DiPirro 1989
Dresner et al. 1986
Dresner 1989

Hermanson et al. 1986
Israelsson et al. 1988
Lee-Ng-Brooks 1988
Mills et al. 1988
Mord et al. 1986
Nast et al. 1986
Ng-Lee-Brooks 1989
Purohit et al 1988
Yang et al. 1980
Yuan-Frank 1988
Yuan-Nast 1987
Yuan-Nast 1988

Table 5.3. Authors of papers on mechanical pumping
systems

Arp 1986
Berndt et al. 1989
Huebener et al. 1984
Izenon Swift 1988
Kamioka et al. 1984
Kamioka 1989
Ludtke et al. 1988
Ludtke-Daney 1988
Staas-Severijn 1969
Walstrom et al. 1988

6. SPACE SYSTEMS FOR He I-He II FLUID PROCESSING

The provocative question has been asked: can Helium-3-Helium-4 dilution refrigerators operate aboard space craft (Jackson 1982)? Similar questions may be raised for other liquid-vapor processing components. Apparently the conversion of terrestrial superfluid liquid He II systems is easy for temperatures below the lambda point. He II has special thermomechanical drive mechanisms. As gravity is absent, the use of the thermomechanics (mechano-calorics) appears to be relatively straightforward. However this first superficial inspection may be misleading. For instance, during high heat loads in terrestrial He II at "1 g" there may be a sufficiently high limit imposed on efficient cooling via vapor bubbles of a nucleate boiling "layer". This mode has been called "triple-phase nucleate boiling". No information appears to be available about the related limits for He II-wetted components at micro gravity. Van der Waals forces and electric fields (e.g. Israelsson et al. 1988) appear to aid in the liquid management tasks.

Careful evaluations may include initial ground tests, and in some cases equipment may be turned upside down in order to check functioning of the device. An example is the VLPS test of Selzer et al. (1970) in the initial experimental evaluation of the Fairbank plug. Drop towers and short duration micro-gravity flights may provide guidance data for the system to be used in space. Design trade studies in various areas have been conducted. Examples are capillary/surface tension devices (Frank et al. 1988, J.M. Lee 1989, Nast et al. 1986, Purohit et al. 1988). Other concerns have been in the following categories: liquid volume and mass losses, power and heat input requirements.

"Passive" liquid pumpdown. Breon (1988) has addressed volumetric liquid losses during fluid handling on the space station. For instance, liquid Helium-4 pumpdown has been calculated for evaporative cooling and for JT-mediated cooldown. In both cases the latent heat of vaporization is utilized. The pressure range covered in the studies corresponds to temperatures from 4.5 K to

1.5 K.

In contrast to terrestrial operations, space provides "vacuum pumping", ideally at zero energy expenditure. Thus, power requirements are not a great concern. However for the overall "economy" liquid preservation is important. The results obtained show a rather small superiority of the JT method in comparison to the evaporative cooling method. Figure 6.1 shows the liquid volume retained as a function of the initial temperature (T_i). The volume is a monotonically increasing function of T . A comparison with Figure 4.1 shows qualitative agreement with the liquid mass retention data (yield [y] results).

Other mass fraction results have been reported in the literature for evaporative cooling (Mironer 1986, Carandang et al. 1986). The comparison of rigorous results with simplifications is shown in Fig. 6.2 from Carandang et al.(1986). It is seen that pumpdown to 1.5 K involves substantial losses. The real vessel has heat inputs, and liquid loss data appear to be in agreement with the role of the "zero heat leak" vessel performance as upper bound. For a quick assessment, the figure of Carandang et al. (Fig. 6 of their paper) is reproduced here as Fig. 6.3.

The Claudet et al. liquid processing system, modified for space, appears to be useful. However as more plumbing, preferably in light-mass aluminum or similar alloy, is added, careful considerations of weight penalties are in order. For the Claudet et al. system we refer to the previous section 4. In summary, the various thermodynamic processing options give thermodynamic constraints whose heat leaks and masses need to be known. All of the options show significant improvements in liquid retention when liquid near the lambda point is supplied.

Active devices, such as space station refrigerators, appear to be of great interest as soon as reliability figures have created confidence along with a good efficiency record.

Vapor-liquid phase separation (VLPS). The VLPS components and subsystems appear to be rather rich in variations tailored for specific vessel operation demands. The porous plug acting

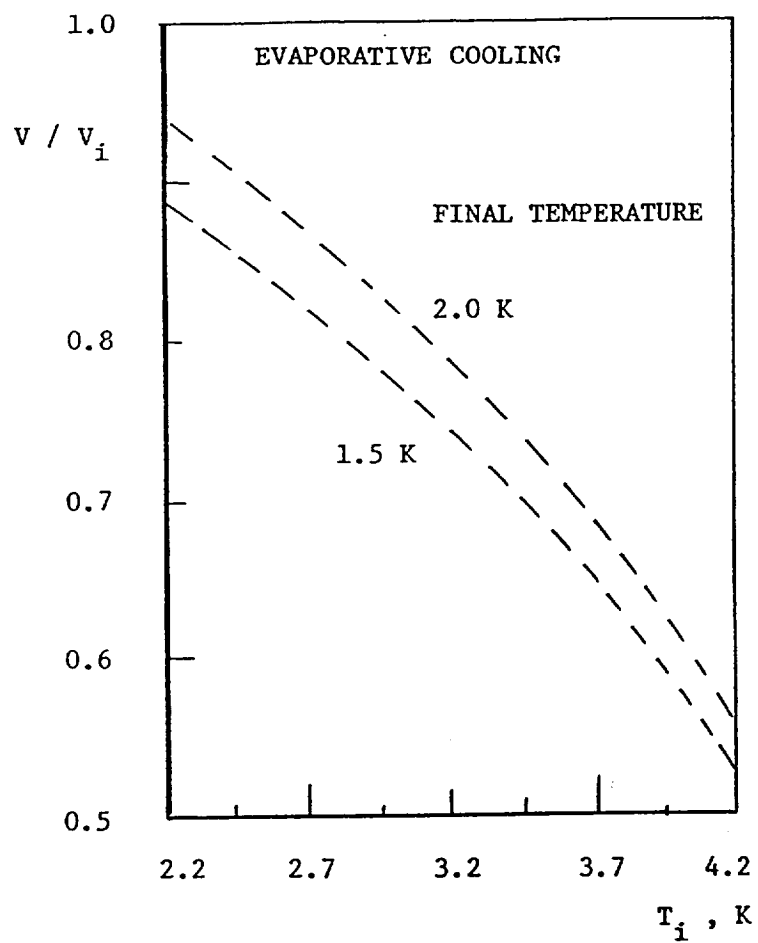


Fig. 6.1 . Volumetric liquid fraction retained as a function of initial temperature T_i ; (Breon 1988) ; parameter : final temperature of evaporative cooling .
 V volume of liquid retained;
 V_i initial volume .

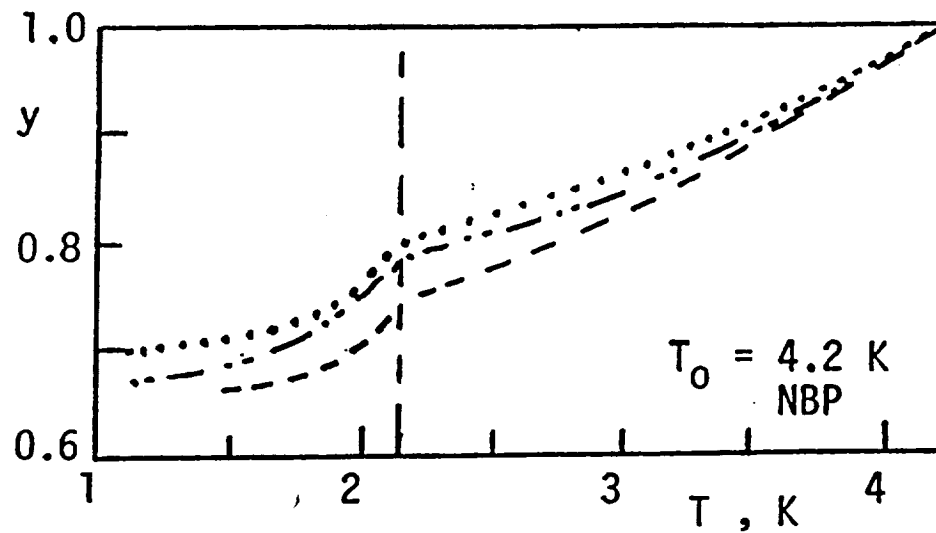


Fig. 6.2 . Comparison of liquid yield predictions for evaporative cooling;
 Starting temperature : $T_i = 4.2$ K (NBP);
 --- simplified equation^{*1};
 ... power law approximation ;
 -.-.-.- Mironer (1986);
 Further details are given in Carandang et al. 1986.

$$*) \quad \lambda \, dm = -m_L \, C_p \, dT$$

$$y = m/m_0 = \exp \left(\int_T^{T_i} -dH/\lambda \right)$$

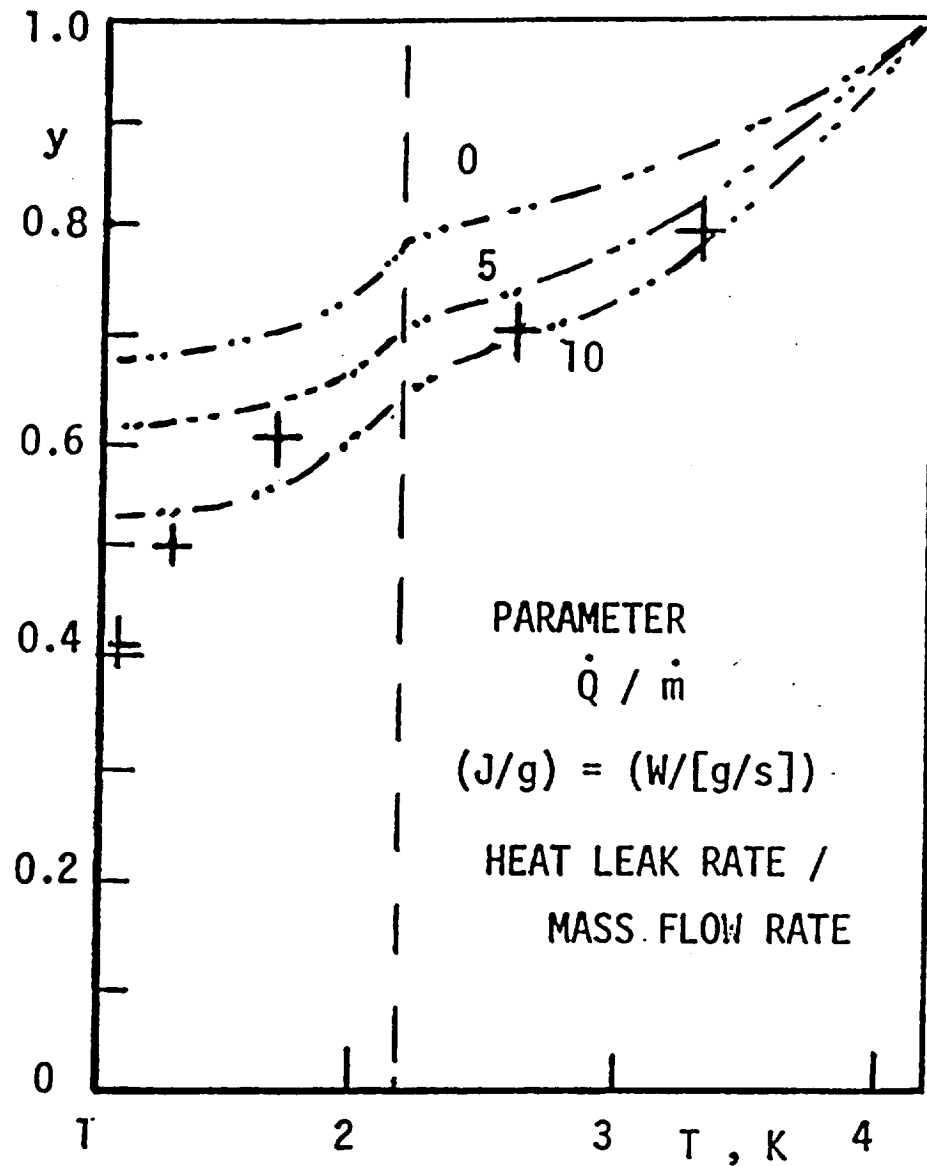


Fig. 6.3. Liquid mass fraction retained (y-value) resulting from pumpdown, starting at 4.2 K, associated with evaporative cooling;
 Parametric result of Mironer (op.cit.);
 Data of glass dewar operation; Basis : J.L. Olsen, as compiled by Carandang et al. (1986).

as "passive device" seems to be the simplest solutions. (This component may be needed in the implementation of the thermodynamics of the preceding section.) It turns out that "active VLPS" operation may include operation on the characteristics toward liquid breakthrough. A downstream vaporizer heat exchanger may be needed, and work of the Klipping group has provided a rich data base for the active slit system with controlled operation (Klipping group: Denner et al. 1978, 1980, 1986; Klipping 1986).

Pore size selection and overall plug size selection has been a topic of great interest, as documented in the literature. The following conclusions seem to be suggested by authors' observations: there is no apparent agreement in throughput versus driving force regime nomenclature; there appear to be difficulties of isolated liquid breakthrough for plugs with cracks and pinholes; certain operational conditions in terrestrial tests suggest vapor penetration from the downstream side of the plug toward the liquid wetted domains. Further permeabilities are not uniquely defined in some cases. Thus, a general comparison based on heat (normal fluid) transport has been less common than to be expected .

Basic understanding of VLPS progress has been forthcoming for IRAS type plugs (porous stainless steel sintered plugs; Urbach Mason 1985). It has been possible find a common frame of reference for the comparison: the "bottleneck" transport mode is caused by normal fluid flow limitations for this class of plugs. As the normal fluid carries the heat, it is the heat flow which is limited by the liquid-filled spaces (Yuan 1985, Yuan et al. 1987, 1989). The location of each plug in the characteristic length diagram forms the basis for an initial critical assessment of a plug manufactured for a specific task.

The literature on VLPS has been quite extensive, and the proceedings of space cryogenics workshops may be useful. Documentation of the workshops has been available since 1986: issues of the "Cryogenics" journal February 1986, January 1987, February 1988, May 1989. The following references are quoted explicitly (in addition to the authors mentioned above: Elsner

1973, Petrac 1975, Karr-Urban 1980, Becker et al. 1980, Schotte-Denner 1981, Murakami 1984 (further Nakai et al. 1984, 1987), Urbach-Mason 1984, Schotte 1984, Karr-Hendricks 1986, Ruediger-Wanner 1987, Schaellig-Seidel 1987 and collaborators.

Transfer line system: thermodynamics and transport. The specifications of the line may include cooldown of warm components at the receiver end and "cold" vessel processing tasks. For both types of pumps, mechanical and fountain effect pump (FEP) devices, a temperature difference appears. Thus, a certain thermodynamic path is representative of the mean fluid state changes. Further, heat inputs are important, and the ideal "zero heat leak" transfer line is an ideal reference case.

Examples of transfer lines have been presented in the various space cryogenics workshops (documented as listed above). A few papers mentioned here are given as follows: Analytical study of He II flow characteristics (Mord et al. 1986, Hermanson et al. 1986, Lee-Ng-Brooks 1988; Snyder 1988, Ng et al. 1988); turbulent flow pressure drop (Walstrom-Weisend-Maddocks-Van Sciver 1988).

Pumping of liquid has been a major concern including the optimum choice of parameters for stationary devices such as FEP systems and other arrangements. Concerning a comparison of mechanical pumps with FEP units, there are entirely different performance concepts. The FEP needs only thermal energy (in principle, being a "waste heat" user). The mechanical pump needs mechanical power, and cavitation at the inlet of rotor systems is a concern, e.g. centrifugal and axial pumps. For FEP units, the initial liquid acquisition has been of great interest.

An initial example of a *comparison* between FEP and mechanical pump has been presented (Arp 1986). Topics of mechanical centrifugal pumps have been addressed by several authors, e.g. Ludtke-Daney 1988, Daney 1988. Additional authors addressing pump phenomena have been Steward (1986), Izenon-Swift (1988), Van Sciver et al. (198), Berndt-Doll-

Wiedemann (1989) and others. Other mechanical means have been pressurization devices, e.g. Kamioka 1989.

Concerning FEP units and related systems, the on-orbit transfer has been of great interest, e.g. Kittel-DiPirro 1989, Kittel 1988 and others. (We refer also to section 5 as far as general FEP use in the "vortex refrigerator" is concerned.)

Liquid acquisition has been a topic of the 1988 space cryogenics workshop (Cryogenics May 1989). For instance, Frank-Yuan (1988), Anderson (1989) and DiPirro (1989) have presented details of acquisition system development work whose design constraints have been discussed by J.M. Lee (1989). Mesh screen use for acquisition has been presented by Maddocks-Van Sciver (1989).

The influence of electric fields for fluid motion control has been of interest in the area of dilution refrigerators (Jackson 1982) and for space cryogenics, e.g. Israelsson et al. (1988).

Non-ideal conditions. The VLPS operation at micro-gravity does not involve a significant static (gravitational) pressure increase. Therefore, the operation is much closer to vapor-liquid equilibrium boundaries, on the liquid side than to ideal thermostatics (Fig. 6.4). A simplified set of idealized state changes is shown in Fig. 6 as changes a to c.

With the establishment of non-ideal conditions the possibility of alternate cooling paths appears to be an interesting area of applications. For instance, the sequence "P- μ " may be considered a part of the cycle of the previous section 5. Non-ideal conditions appear to be a realistic possibility.

For non-ideal FEP systems, Kittel (1988) has treated the iso-caloric pump including a two-stage FEP version.

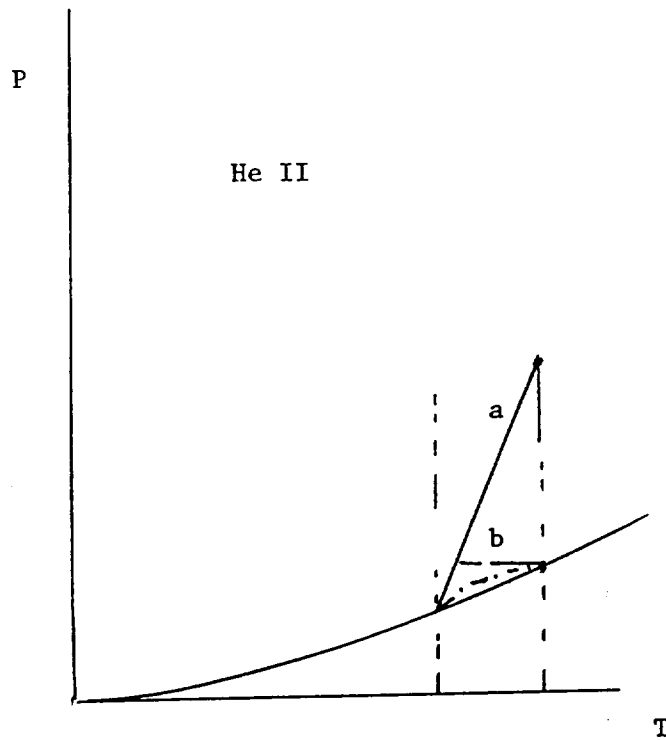


Fig. 6.4 . Phase diagram with changes of state, schematically;
 a. ideal case of $d\mu = 0$;
 b. idealized change with a small P-increase at $d\mu = 0$
 and a subsequent isobaric change;
 c. change near vapor - liquid equilibrium

7. EXPERIMENTS

The experiments conducted include the following tasks: permeability determination at room temperature using both sintered ceramics and metal porous media, pressure transducer measurements at room temperature and at low temperature, test rig construction for the different porous media, test chamber system and component manufacturing for the mechano-caloric test.

Porous alumina. The Al_2O_3 product has been manufactured by Coors Porcelain Company, Golden, CO. Filtration ratings are the usual characterization quantities for separation tasks. For the very fine plugs these ratings vary from one batch to the next with a concomitant shift in spectral distribution. Pore sizes have been quoted to be in the range of $<0.5 \mu\text{m}$. There is a characteristic length diagram: lengths are rather well defined if there are no hollow spaces, and when the plug has a rather uniform porosity distribution (Khandhar, 1989). The ratio of the filtration rating size (nominal size) S_o to the characteristic length (L_c) is about 2-5 for porosities from 30 to 50%. The characteristic length $\kappa^{1/2} = L_c$, for $S_o = 0.2 \mu\text{m}$, turns out to be as small as 0.1 to $0.04 \mu\text{m}$ (or less). This implies Darcy permeabilities at or below 10^{-10} cm^2 .

At room temperature any external application of a pressure difference across the porous medium amounts to a rather low flow in comparison to VLPS plugs. Therefore the geometry chosen is a cylindrical cup-like porous system whose dimensions are not exactly constant along the cup axis. The cup length is 7.92 cm (diameter 1 in = 2.54 cm; wall variation bottom wall about 0.33 cm, side walls about 0.42 cm thick, i.e. the top section has 1.77 cm I.D.). The system used for initial pressure transducer calibration is shown as Figure 7.1. We are indebted to Dr. Elsner for his input and special design, construction and experimental evaluation. Only one complete cup of the two-cup system (number 1) is shown in Figure 7.1.

A similar double cup arrangement has been constructed as test rig for low temperature runs in liquid He II. This system (no. 2) is shown schematically in Figure 7.2. A phenolic ring section serves as cup connector with current leads for an internal heater and a thermometer (s). In contrast to the first system, a copper shielding cylinder is absent. The assembly is mounted on

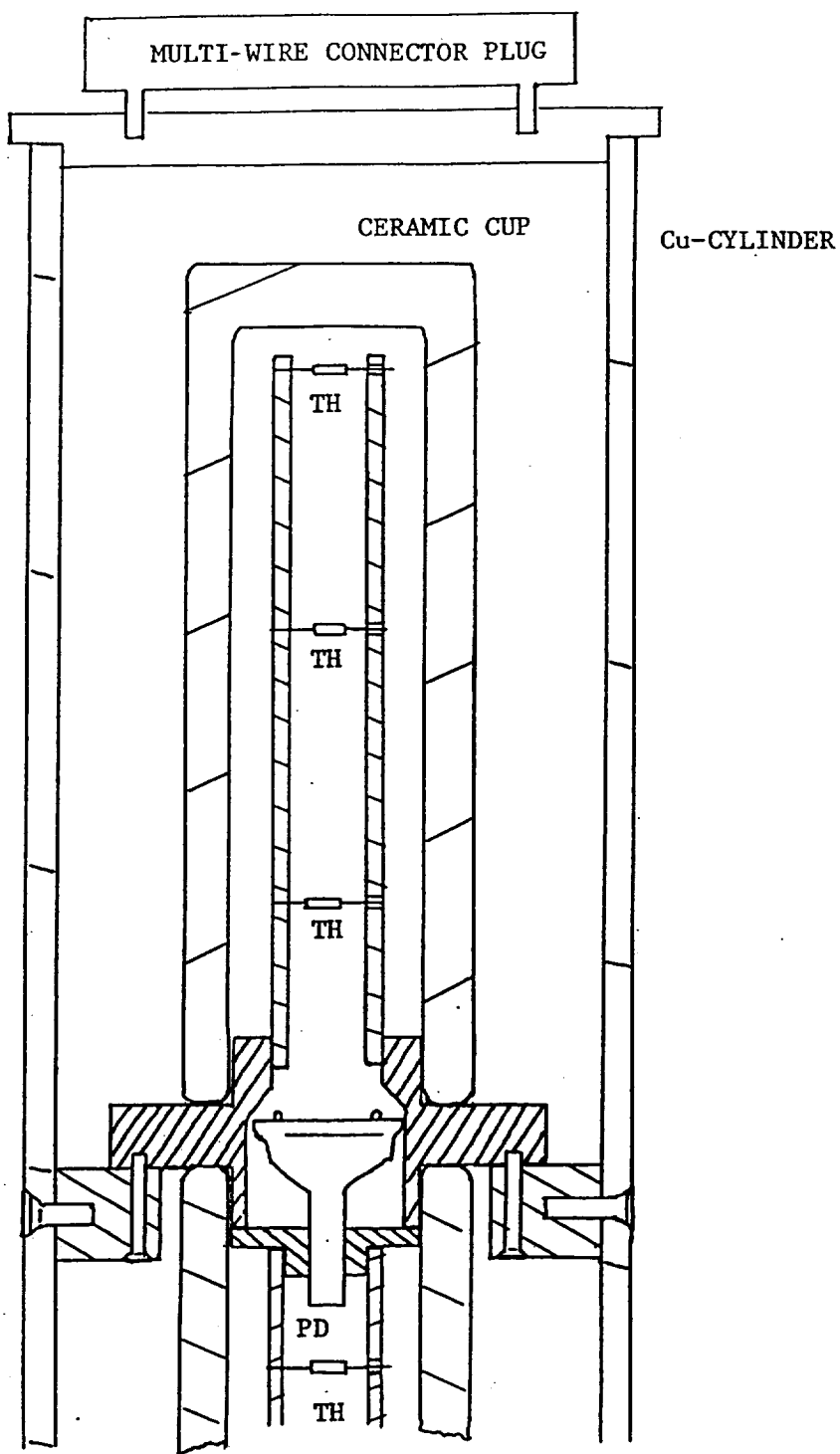


Figure 7.1 . Ceramic double-cup assembly : apparatus # 1;
PD pressure transducer ; TH thermometer .

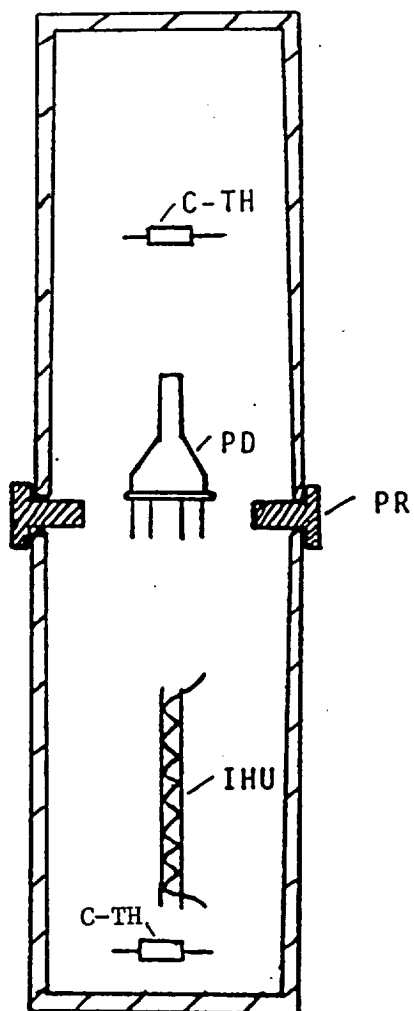


Fig. 7.2. Ceramic porous filter cup system (apparatus # 2); Schematic drawing; C-TH carbon thermometer; IHU internal heater unit; PD pressure transducer; PR phenolic ring .

a phenolic disk located at the bottom of the two-cup assembly. Various wires coming out from the interior, through the phenolic ring, are routed to a multi-wire connector plug. The wire system, wound in a helical fashion around the support tube, provides connection to instruments outside the helium dewar.

Room temperature permeability. Helium gas is passed through the system using a simple "outflow method". A single cup sample is subjected to flow from a helium gas-filled balloon attached, after filling, to the open side of the cup. The outflow takes place slowly, at room temperature and for near-ideal gas conditions $P = \rho RT$. Thus, we have $VdP + PdV = 0$, or an absolute relative change in pressure

$$\Delta P/P \approx -\Delta V/V \quad (7.1)$$

The flow rate is accessible from observations of the rate of change of the volume with time, e.g. by order of magnitude: $1 \text{ cm}^3/\text{s}$. According to Darcy's law the volumetric flow rate is

$$\dot{V} = A_{\text{TOT}} v_o = A_{\text{TOT}} [|\Delta P|/d]/\eta \quad (7.2)$$

From Eq. (7.1) the pressure difference is obtained to first order as $\Delta P \approx P(\Delta V/V)$. Therefore, the permeability is obtained as

$$\kappa = \eta(\dot{V}/\Delta P)d/A_{\text{TOT}} \quad (7.3)$$

The order of magnitude is estimated as follows:

Shear viscosity, Helium-4:	200 μP ;
Pressure:	1 bar;
Thickness (d):	0.4 cm;
Total area (A_{TOT}):	10 cm ² ;
Relative volume change:	0.1;
Resulting permeability (apparent):	10^{-11} cm^2 .

(order of magnitude result). Numerical values during the outflow test have been based on the

mean area of $A_{\text{tot}} = 56 \text{ cm}^2$ and the thickness $d = 0.4 \text{ cm}$. The radius of the balloon, filled with Helium-4 gas, varies with time (Fig. 7.3). The plot shows an initial change of the radius with time corresponding to 0.2 cm/min . The volume flow rate is $\dot{V} = 5.9 \text{ cm}^3/\text{s}$. The relative volume variation during the initial observation is $\Delta V/V = 0.3$. The result is an apparent permeability of $2.4 \times 10^{-11} \text{ cm}^2$. There is a mean free path (MFP) effect causing slip at the narrow fluid passages of the porous medium.

The mean free path effect is taken into account on the basis of the modified Knudsen equation proposed recently by us for sintered metal plugs (Frederking et al. 1988). Figure 7.4 is reproduced from the previous work. It is seen that the slip effect is quite large for permeabilities on the order of 10^{-11} cm^2 . The individual gas constant is referred to (Fig. 7.4): R is the universal gas constant divided by the molecular mass (molecular weight M of species i). The MFP is based on the definition used in vacuum technology (Barron 1985). [Helium gas at room temperature, 1 atm: $\text{MFP} = 195 \text{ }\mu\text{m}$. Figure 7.5 shows MFP-values at 1 atm and 293 K for various simple gases.

The variation of the effective permeability with MFP-to-characteristic length ratio is based on the function for the sintered metal plugs. The permeability for infinitely small MFP (bulk fluid medium) turns out to be $1.4 \times 10^{-12} \text{ cm}^2$. This value is comparable, in order of magnitude, to the ceramic cup result reported by DiPirro (1988), [$4.43 \times 10^{-12} \text{ cm}^2$; subcooled He I result]. The cup has been from the same manufacturer (Coors).

Metal Flow Restriction Device

Permeability. A disk-screen system has been used in order to provide an alternate solution with only metallic components (exception: epoxy wall sealing). The main "throttling device" is a Cu-disk with fine crack-like "holes". There are wire screen spacers between the disks. The screens of circular form, matching the disk diameter, have been cut from stainless steel 304 cloth. The wire

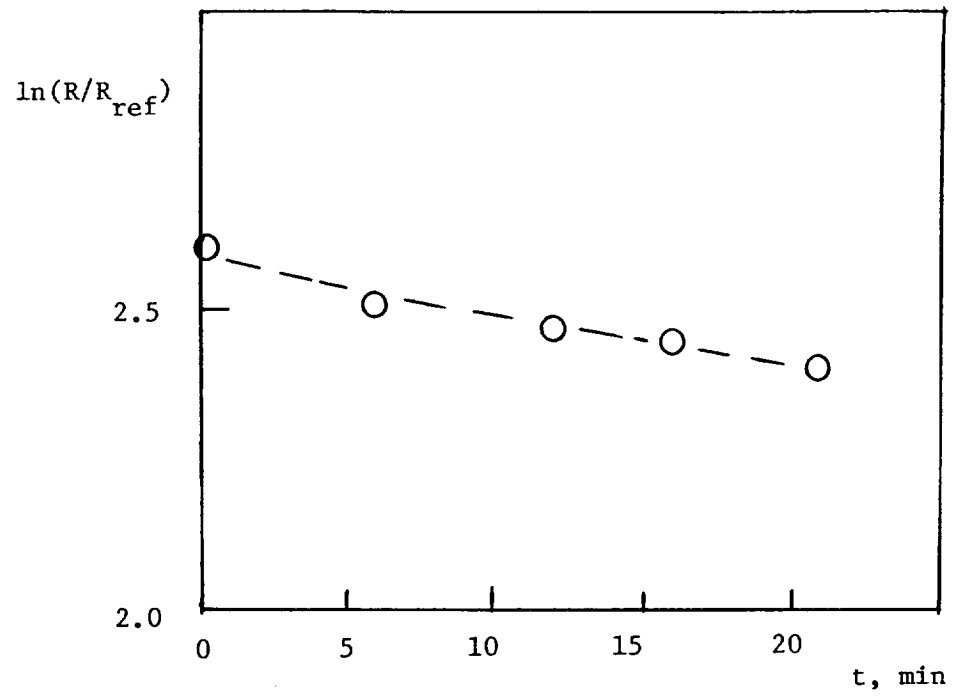


Fig. 7.3. "Outflow test" : Radius ratio in logarithmic units
as a function of time ;
 R_{ref} = reference radius = 1 cm

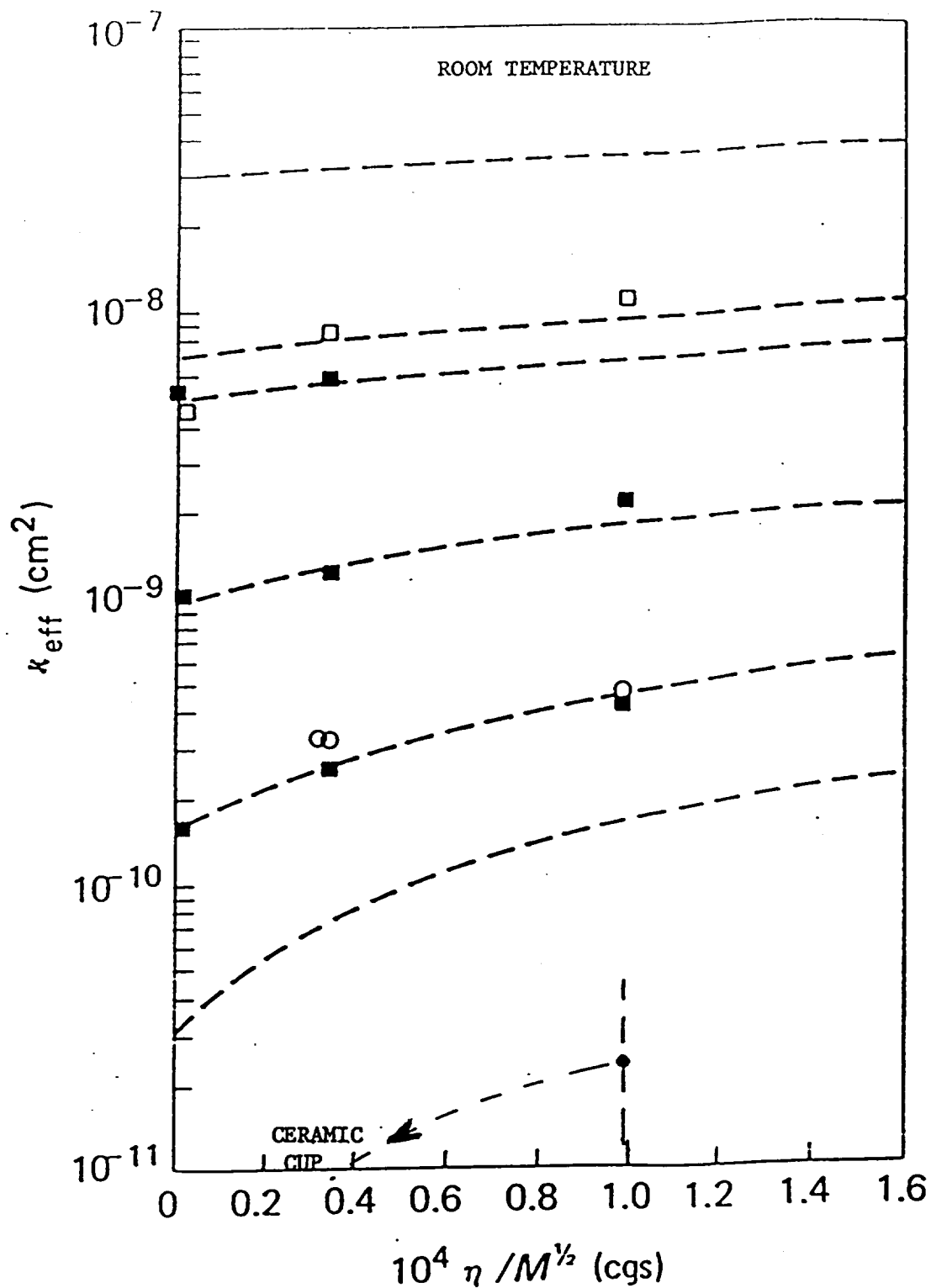


Fig. 7.4 Effective permeability associated with slip caused by mean free paths exceeding fluid passage spacing;
(from "Cryogenics" vol. 28, 1988, 110);
--- modified Knudsen equation of above ref.; $k_{eff} = \alpha \cdot f$;
function $f = [1 + 1.15 \frac{MFP}{L}]$; $L = \alpha^{1/2}$;
MFP = mean free path = $\sqrt{\frac{\pi}{2}} \frac{c}{(h/P)} (R_1 T)^{1/2}$; $R_1 = 8/M_1$;

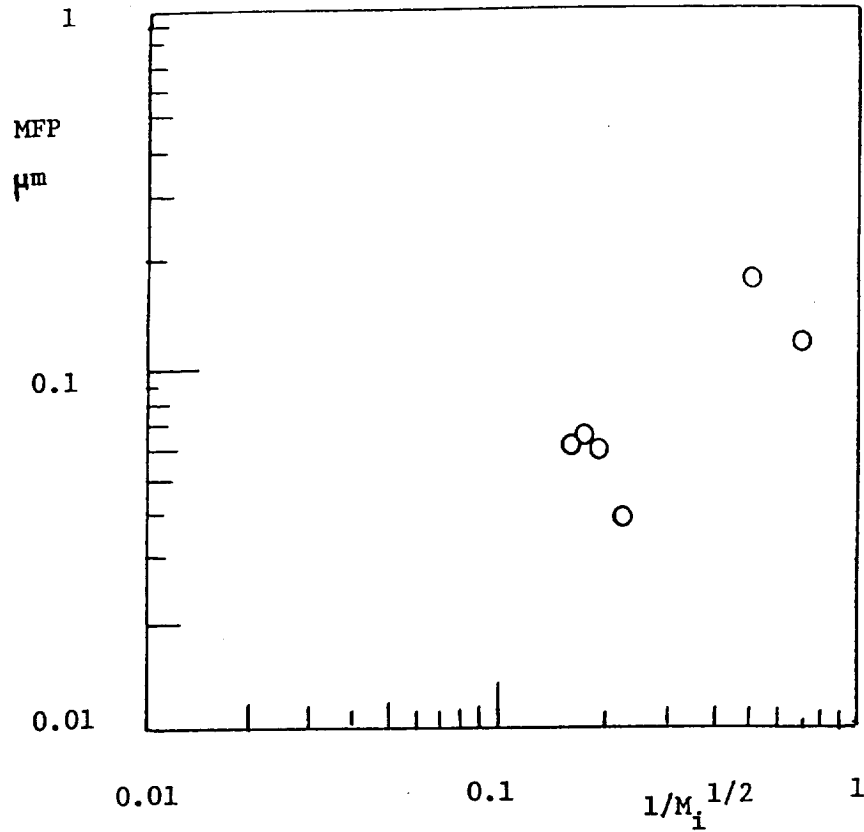


Fig. 7.5. Mean free path (MFP) values at 1 atm and 293 K for various light gases as a function of $M_i^{-1/2}$; M_i molecular weight (molecular mass) of species i .

MFP of Barron (op. cit.) used in vacuum technology:

$$\text{MFP} = 8.6 \times 10^3 (\eta/P) (T/M_i)^{1/2};$$

η shear viscosity, Poise = g/(cm s)

P pressure, micron Hg

T temperature, K

M_i g/mol

MFP cm

mesh has a square weaving pattern. The nominal wire diameter is 1 mil (25.4 μm) ["500 mesh"]. From this nominal number one calculates a nominal "square hole" diameter of 25.4 μm . The porosity of the material is about (2/3).

The Cu-disks have a diameter of 9 mm. Along the circumference there is a rim domain without holes. The holes have sizes varying from several microns across the narrow side of the passage to about 10 μm in the elongated direction.

Room temperature runs with Helium-4 gas show a linear pressure drop versus throughput function. There appears to be a small slip effect which is considerably reduced compared to the double cup alumina system. The individual copper disk permeability is related to the approach conditions toward the perforated disk. Values from 5×10^{-9} to $9 \times 10^{-9} \text{ cm}^2$ have been found for two sample disk assemblies. The disk-screen spacer setup has 10 Cu-disks and 9 stainless steel spacers. Figure 7.6 is a plot of the pressure drop versus the velocity at room temperature. The permeability, uncorrected for mean free path effects, is $5.85 \times 10^{-8} \text{ cm}^2$.

Cryostat system. A schematic picture of the cryostat assembly is given as Figure 7.7. Helium-4 gas from a gas cylinder is admitted to a liquid nitrogen precooler. The gas flows through a partially insulated transfer tube into the helium dewar sections of heat exchanger packages. The mechano-caloric can is equipped with the incoming fluid line, the outflow line and vacuum line. The gas leaving passes through a downstream flow meter.

Figure 7.8 is a schematic graph of the chamber with a U-shape loop and the mechano-caloric plug section in the upstream leg of the "U". The top components near the fluid entrance are shown as Figure 7.9. The top is a Cu-disk. Past use of coupling heat exchangers on vacuum insulated cans has included "pigtail" heat exchangers: a small Cu-tube helix, open-ended on both ends permits an easy mounting technique by brazing (or equivalent bonding technique). Pressure transducer results.

Initial data have been taken at room temperature and liquid nitrogen tempera-

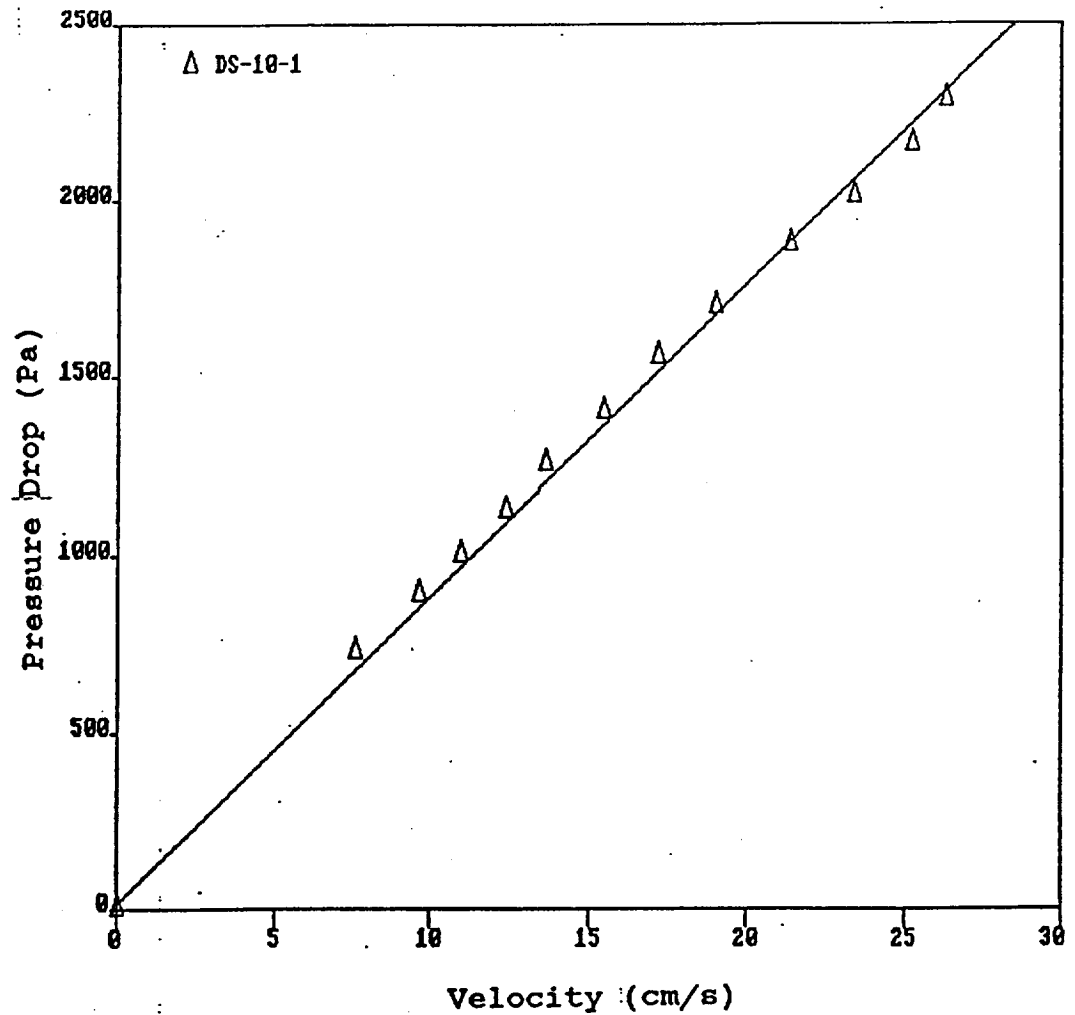


Fig. 7.6. Pressure difference versus velocity for disk-screen system : 10 Cu-disks , 9 stainless steel creen spacers; Helium-4 gas at room temperature near 1 atm.
The velocity is based on the total ("active") area of the disk which has perforated holes .

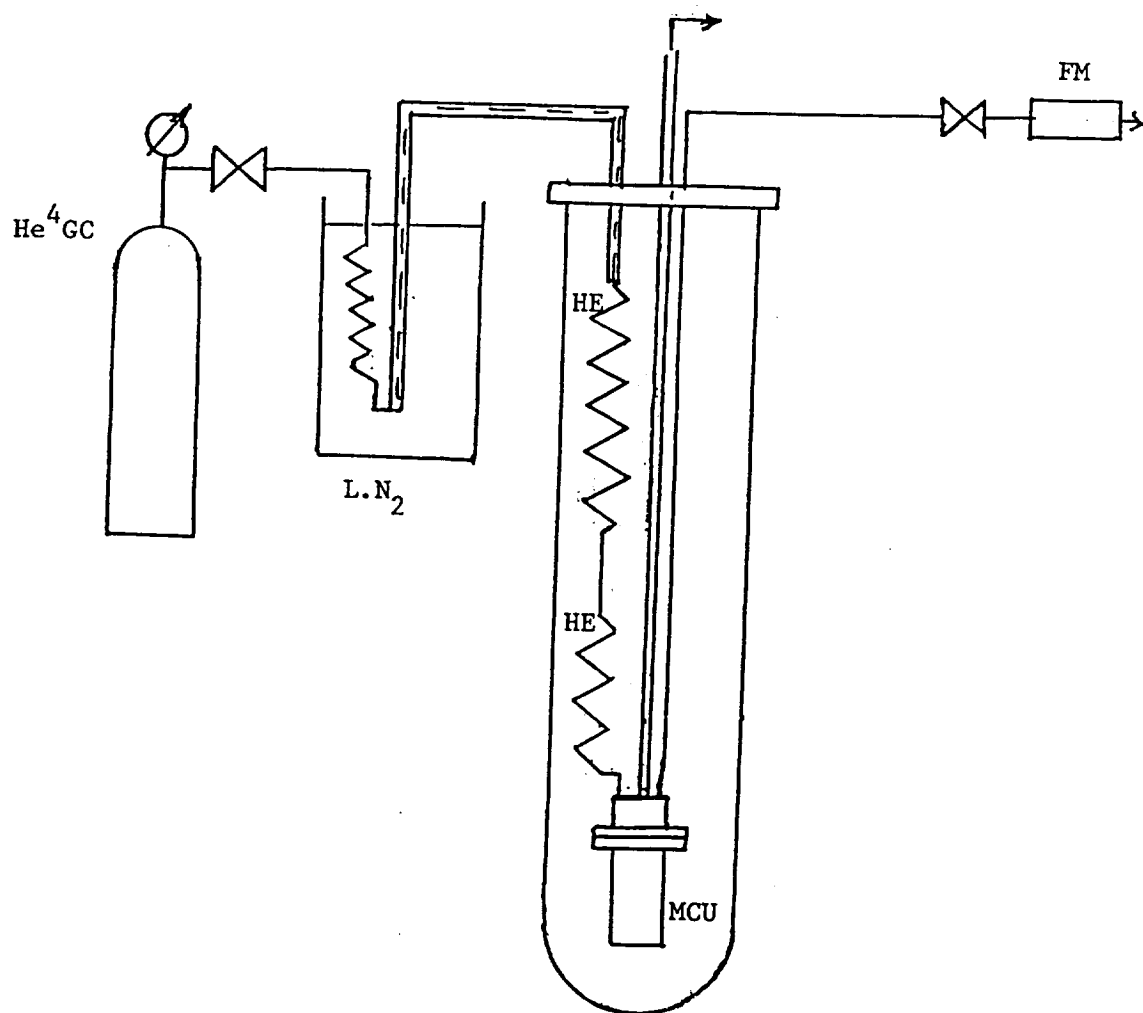


Fig. 7.7. System setup for He II near 1 atm ;
 FM flow meter ; HE heat exchanger ; He^4 GC gas
 cylinder for He^4 ; L.N_2 liquid nitrogen pre-cooler bath ;
 MCU mechano-caloric unit .

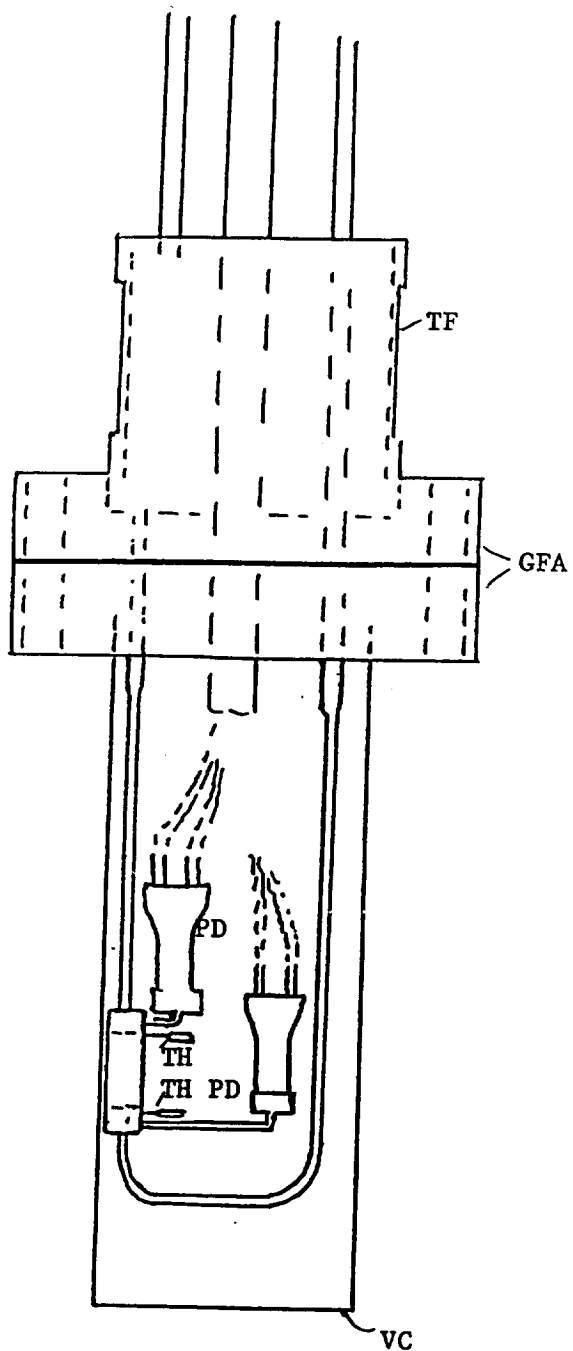


Fig. 7.8. Mechano-caloric He II_p system setup , schematically;
 GFA gasket flange assembly ; PD pressure transducers;
 Th thermometers ; TF top fluid chamber for He II_p;
 VC vacuum can .

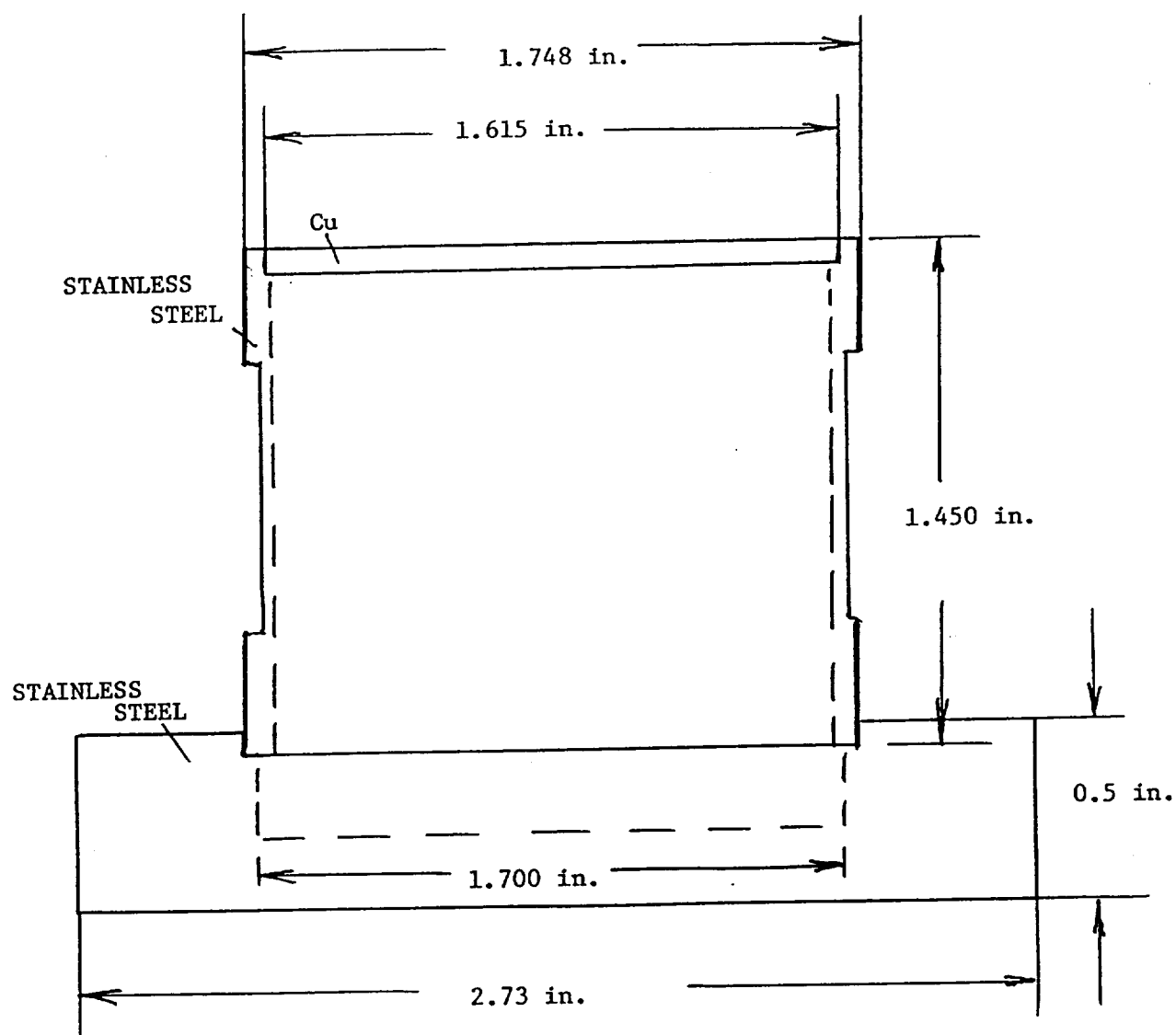


Figure 7.9. Top section of the apparatus for He II_p near and above atmospheric pressure : pressure chamber with top Cu-plate and standard flange for Cu-gasket serving as seal between He II_p and vacuum .

ture with the alumina apparatus no. 1 (courtesy Dr. Elsner). The pressure transducer of the KPY series (Breimesser et al. 1984 and Walstrom et al. 1987) has been selected. Though originally the transducer operation has been specified only for the temperature range from -40°C to $+125^{\circ}\text{C}$, low temperature use appears to be useful. Figure 7.10 presents data obtained at various bath and environmental conditions. The dissipation through the system is rather high: the resulting thermal load from the instrument may be used for heat input purposes.

Figure 7.11 shows thermogram records of apparatus no. 2. Figure 7.11a displays the thermometer response to a step input in power. The linear region is seen to be followed by non-linear transport conditions. Fig. 7.11b shows the corresponding pressure transducer results. The linear and non-linear parts of the T-records are seen to be reflected in the pressure readings.

An example of a high step power input is presented as Figure 7.12. The temperature excursion after the initial T-rise corresponds to "high" temperatures of film boiling (Fig. 7.12a). The conditions are locally not quite uniform: Fig. 7.12b shows an initial pressure rise, however the subsequent P-history tends to be uniformly high while the temperature fluctuates significantly.

An inspection after the liquid Helium run with system #2 revealed inconsistencies of the data in comparison to previous work with sintered stainless steel plugs. After warmup to room temperature alumina cup damage was found. Cracks appeared, and chips of alumina had been flaking off at an unknown point in the history of cup operation. Afterwards, closing of the crack and damaged domains by epoxy was part of the preparation of a second set of runs. It turned out that the same phenomena did show up again: cracks again obscured the approach toward a low temperature permeability determination of the alumina.

Comment. The work at this point has been facing the demanding task associated with preparations of the dual conference CEC/ICMC'89 at UCLA, July 24-28, 1989. The great success of the

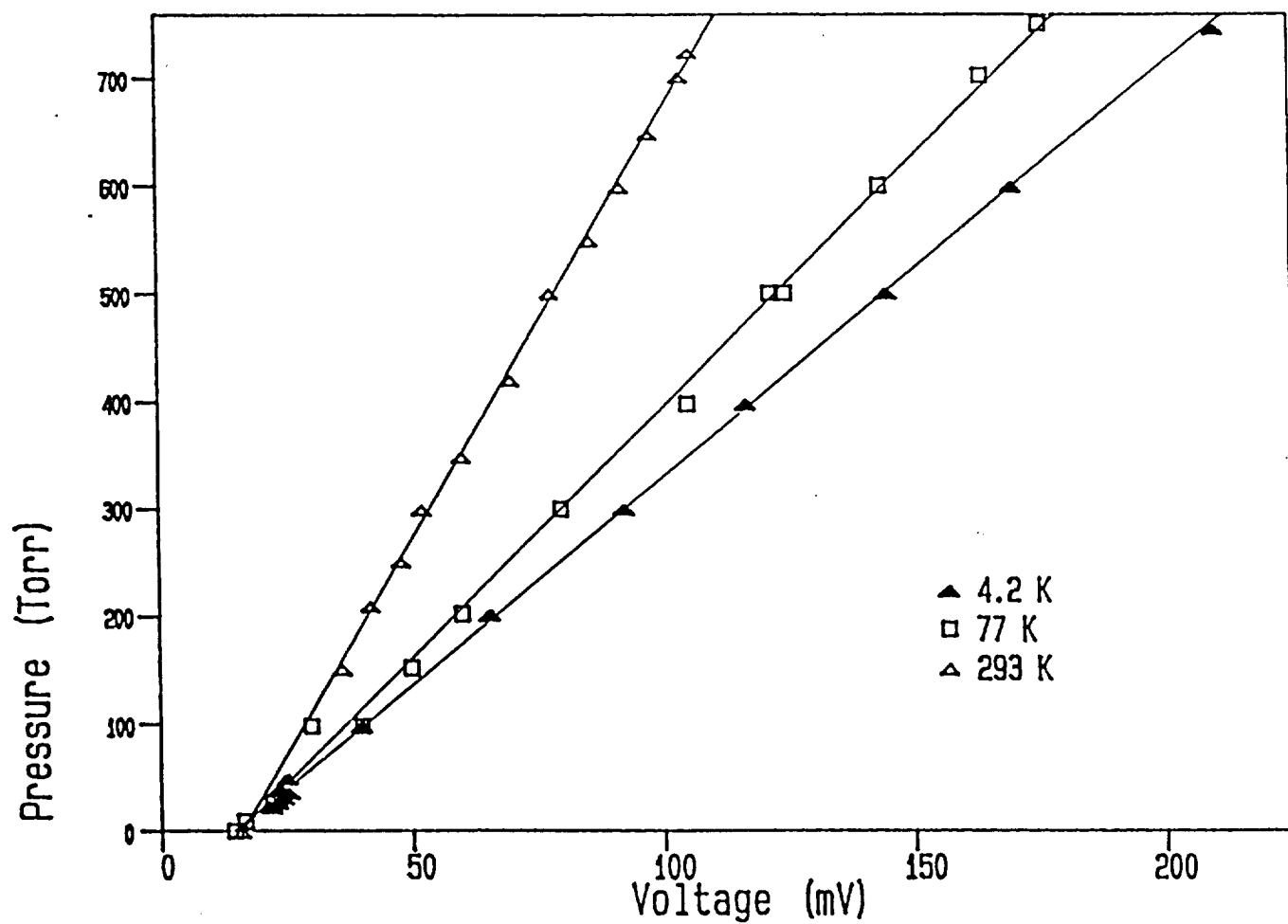


Fig.7.10. Pressure transducer characteristics at different bath temperatures.

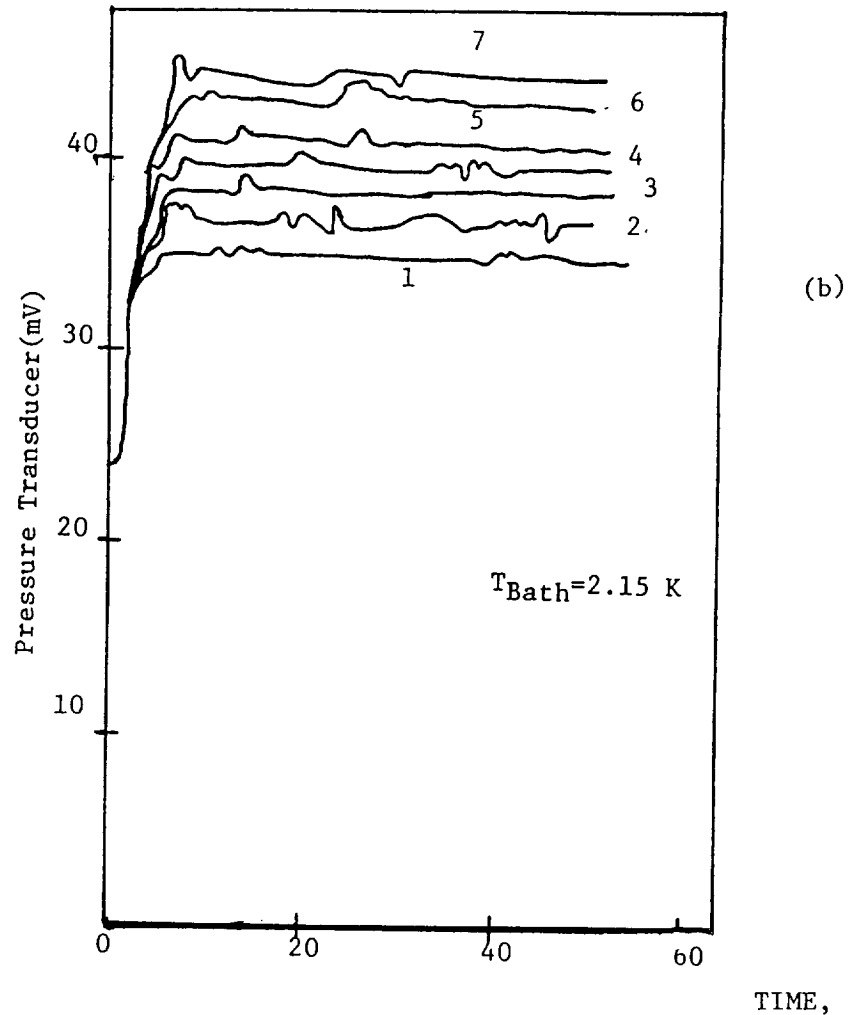
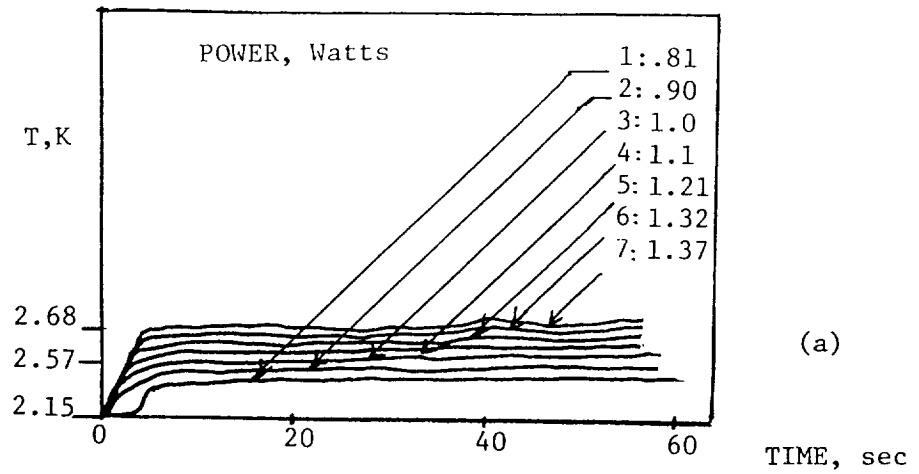


Fig. 7.11 Thermograms resulting from step power input to heater located inside porous cup assembly (apparatus # 2);
a. Thermometer response (T : non-linear scale of C-thermometer voltage) ;
b. Pressure transducer signals .

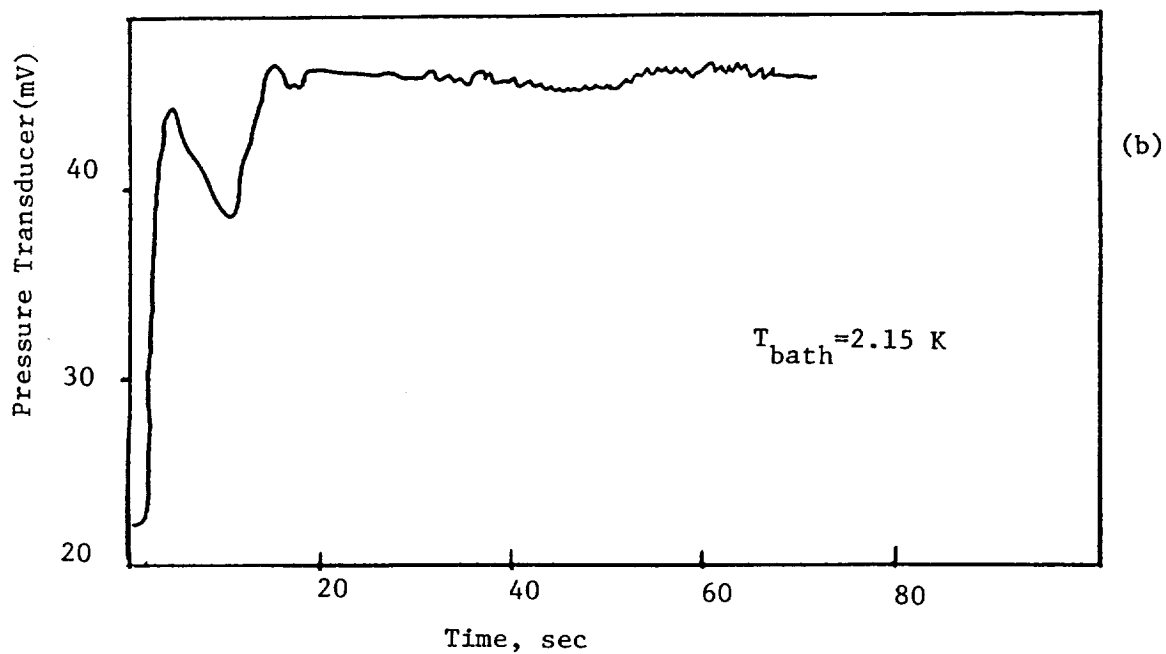
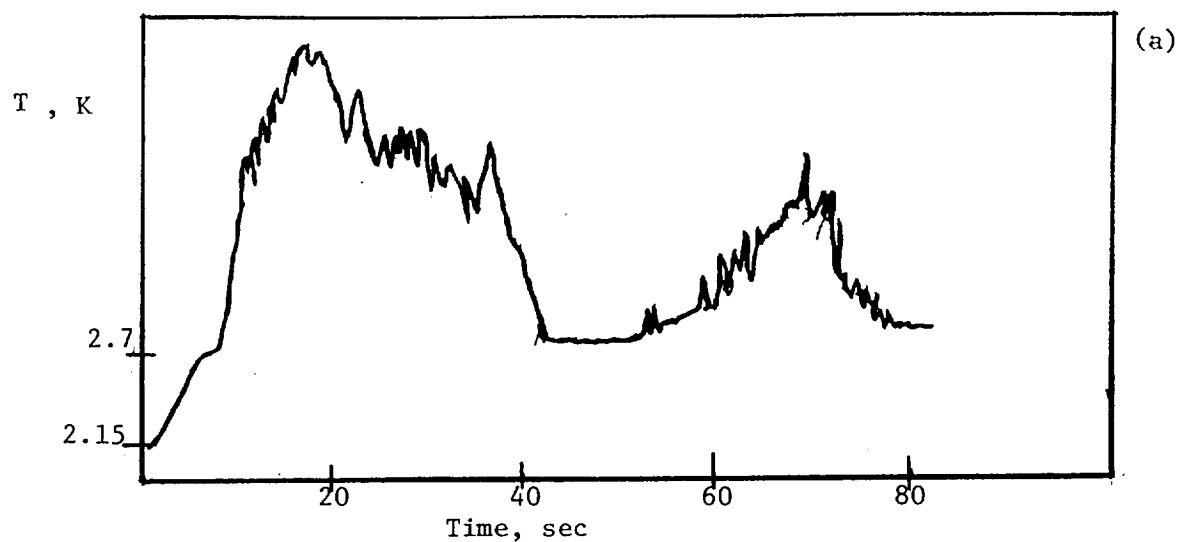


Fig. 7.12. Thermogram example for high step power input leading to local vapor film formation ; Power: 1.69 W ;
a. Thermometer signal (voltage units, i.e. non-linear T-scale);
b. Pressure transducer signal.

conference with more than 800 attendees has been possible by the support of many people. The present lab crew has provided devoted input and great help while the P.I. has been CEC chair. The work carried out so far has provided an initial start for detailed tests of various "expansion" components. Acknowledgments are certainly in order : Gene Kim did a fabulous job during machining, construction and assisting with data collection. Steve Novak, and Foster Tam have provided enthusiastic support throughout the 1988/1989 time period up to now.

8. CONCLUSIONS

In the area of mechano-caloric (MC) effect applications, such as "MC-device" subsystems of He II vortex refrigerators, the following research results are listed for the present work:

The coefficients of performance are high in the high temperature range of He II. At low T, the competition between heat leakage and high cooling coefficients constitutes an ultimate limit imposed on vortex refrigerator use. For space cryogenics, the task of interfacing a He I system with a He II refrigerator appears to be somewhat similar to terrestrial choices if a dual pressure system is employed (sacrificing simplicity). (Note: reliability and simplicity may impose constraints on sophisticated solutions.)

In the area of other MC applications and related systems there are special tasks, e.g. liquid transfer lines. The following results appear to be suggested by our studies: The selection of a "half-cycle", consisting of an isobar followed by an isopotential change ($P-\mu$) is attractive from the point of view of ideal thermodynamics. Realistic micro-gravity work faces non-ideal conditions. The use of the heat ($T S$), in principle, is less attractive for passive systems compared to the latent heat of vaporization as the latter is large compared to the former. These points appear to make the distinction between (μ -P) and VLPS less clear cut in microgravity. The suggested version is the (μ -P) half cycle device for certain cooling/heat rejection tasks.

In the area of experimental results, the data show the usefulness of various permeability measurement techniques and precautions needed for non-metallic components: A very simple version for very low permeability plugs is the outflow method in conjunction with the modified Knudsen equation (a low-T verification is desirable though). The above method appears to be quite handy for initial plug screening purposes. In contrast to compressional loads, the application of tensile stress on ceramics may lead to local fracture in particular when thermal stresses are superposed.

REFERENCES

- Andersen, J.E., *Cryogenics* 29, 1989, 513.
- Arp, V., *Cryogenics* 26, 1986, 103.
- Arp, V. and K. Agatsuma, *Int. J. Thermophys.* 6, 1985, 63
- Barron, R.F., *Cryogenic Systems*, 2nd Ed. Oxford Univ. Press, 1985.
- Becker et al., *Proc. ICEC-8, Genova*, 1980, p.22
- Berndt, H., R. Doll and W. Wiedemann, *CEC/ICMC'89*, July 1986 UCLA, paper DF-O2.
- Biltcliffe, M.N., P.E. Hanley, J.B. McKinnon and P. Roubeau, *Cryogenics*, 12, 1972, 44.
- Bon Mardion, G., G. Claudet and G.C. Vallier, *Proc. ICEC-6, Grenoble*, 1976, p.159.
- Breon, S.R. *Cryogenics*, 26, 1986, 68.
- Brooks, W.F., *Cryogenics* 26, 1986, 61.
- Broulik, B.M. and G.B. Hess, *Phys. Letters* 94B, 1978, 169.
- Carandang, R.M. and T.H.K. Frederking, *AIChE Sympos. Ser.* 251 vol. 82, 1986, p. 63.
- Caspi, S., *AIChE Sympos. Ser.* 224, vol. 79, 1983, p. 84.
- Castaing, B., B. Hebral and A. Lacaze, Heat and mass transfer at low temperatures , in "Heat and mass transfer in refrigeration and cryogenics", eds. J. Bougard and N.H. Afgan, Hemisphere, Wash. 1987, p. 487.
- DiPirro, M. and S. Castles, *Cryogenics* 26, 1986, 84.
- DiPirro, M. and P. Kittel, *Adv. Cryog. Eng.* 33, 1988, 893.
- DiPirro, M. and R.F. Boyle, *Adv. Cryog. Eng.* 33 1988, 487.
- DiPirro, M., *Cryogenics* 29, 1989, 517.
- Elsner, A., Helium flow through filters, *Adv. Cryog. Eng.* 18, 1973, 141.
- Elsner, A. and G. Klipping, *Adv. Cryog. Eng.* 14, 1969, p. 416, vol. 18, 1973 p. 317.
- Elsner, A., *Cryogenics* 27, 1987, 317.
- Frank, D.J. and S.W.K. Yuan, *Cryogenics* 27, 1988, 126.
- Frederking, T.H.K., P. Kittel, T.C. Nast and C.K. Liu, *ICEC-11*, 1986, p. 323.
- Frederking, T.H.K., H.H.D. Tran and R.M. Carandang, *Proc. 4th Intern. Cryocooler Conf.*,

- Easton, MD, 1987, p. 147.
- Frederking, T.H.K., W.E.W. Chen and S. Caspi, IEEE Trans. Magn. 24, 1988, p. 1117.
- Green, M.A., Cryogenics 29, 1989, 484.
- Hakuraku, Y. and H. Ogata, Cryogenics 23, 1983, 291
- Heijden, J.G., W.J.P. De Voogt and H.C. Kramers, Physica 59, 1972 ,473.
- Hendricks, J.B., CEC/ICMC'89, UCLA 1989, paper DB-O1.
- Hendricks, J. B. and G.R. Karr, ICEC-10, Helsinki, 1984, p. 507.
- Hendricks, J.B. and G.R. Karr, Cryogenics 27, 1987, 49.
- Hermanson, L.A. , A.J. Mord and H.A. Snyder, Cryogenics 26, 1986, 107.
- Hofmann, A., ICEC-11, Berlin, 1986, p. 306.
- Hofmann et al., ICEC-11, Berlin, 1986, p. 312.
- Hosoyama K., et al. Jap. J. Appl. Phys. 21, 1982, 1711.
- Huebener, J, G. Krafft , W. Lehmann and J. Minges, ICEC-10, Helsinki, 1984, p. 574.
- Huang, B.J., Cryogenics, 26, 1986, 475.
- Israelsson, U.E., H.W. Jackson and D. Petrac, Cryogenics 28, 1988, 120.
- Izenon, M.G. and W.L. Swift, Cryogenics 28, 1988, 90.
- Jager, B., G. Bon Mardion , G. Claudet and M. Desmaris, Cryogenics 25, 1985, 578.
- Kamioka Y. et al., ICEC-10, Helsinki 1984, p. 578.
- Kamioka, Y., CEC/ICMC'89, UCLA July 1989, paper FD-12.
- Karr, G.R. and E.W. Urban, Cryogenics 20, 1980, 266.
- Karr, G.R. and J.B. Hendricks, Cryogenics 26, 1986, 115.
- Kasthuriengan, S., U. Schotte, H.D. Denner, Z. Scuecs and G. Klipping, Cryogenics, 25, 1985, 518.
- Kasthuriengan, S., H.P. Kramer and A. Hofmann, paper C4.1 presented at ICEC-12, Southampton 1988.
- Kittel, P., AIAA-85-O959, Williamsburg, June 1985.
- Kittel, P., ICEC-11, 1986, 317.

Kittel, P., Adv. Cryog. Eng. 33, 1988, 466.

Klipping, G., Adv. Cryog. Eng. 31, 1986, 851.

Kreitman, M.M. Rev. Sci. Instr. 40, 1969, 1249.

Kreitman, M.M. Adv. Cryog. Eng. 16, 1971, 282.

Ladner, D.R., Proc. Space Helium Dewar Conf., Huntsville, AL, Aug. 1983, p. 231.

Lee, J.H., Y.S. Ng and W.F. Brooks, Cryogenics 28, 1988, 81.

Lee, J.M., Cryogenics 29, 1989, 523

Ludtke, P.R., D.E. Daney and W.G. Steward, Adv. Cryog. Eng. 33, 1988, 515.

Ludtke, P.R. and D.E. Daney, Cryogenics 28, 1988, 96.

Lue, J.W., J.R. Miller, P.L. Walstrom and W. Herz, Adv. Cryog. Eng. 27, 1982, 785.

Maynard, J., Phys. Rev. B 14, 1976, 3868.

McCarty, R.D. , NBS Tech. Note 631, Nov. 1972.

Mills, G.L. et al. Adv. Cryog. Eng. 33, 1988, 497.

Mironer, A. Cryogenics 26, 1986, 69.

Mord, A.J. et al., Cryogenics 26, 1986, 46.

Murakami, M., Proc. Space Cryog. Workshop Berlin, 1984, p. 70.

Nakai, H., M. Murakami and N. Ichikawa, ICEC-10, Helsinki 1984, p. 511.

Nakai, H. and M. Murakami, Cryogenics 27, 1987, 442.

Nast T.C. et al., Cryogenics 26, 1986, 78.

Ng, Y.S., J.H. Lee and W.F. Brooks, J. Thermophys., 1988, 203.

Petrac, D., Proc. LT-14, 1985, vol. 4, p. 33.

Petrac, D. and P.V. Mason, ICEC-8, 1980, Genova, p.97.

Purohit, G.P. and L.D. Loudenback, AIAA-88-2919, 1988.

Roubeau, P., C.R. Acad. Sci. Paris, vol. 273, No. 14, 1971, p. 581.

Ruediger, H. and M. Wanner, Cryogenics 27, 1987, 38.

Schaellig, R. and A. Seidel, Cryogenics 27, 1987, 42.

- Schmidtchen, U. and H.D. Denner, *Cryogenics* 27, 1987, 35.
- Schotte, U., *Cryogenics* 24, 1984, 536.
- Schotte, U. and H.D. Denner, ICEC-8, Genova, 1980, p. 27.
- Schotte, U. and H.D. Denner, *Z. Phys. B* 41, 1981, 139.
- Selzer, P.M., W.M. Fairbank and C.W.F. Everitt, *Adv. Cryog. Eng.* 16, 1970, 227.
- Severijns, A.P., *Cryogenics* 20, 1980, 115.
- Srinivasan, R. and A. Hofmann, *Cryogenics*, 25, 1985, pp. 641 and 652.
- Staas, F.A. and A.P. Severijns, *Cryogenics* 9, 1969, 422.
- Steward, W.G. *Cryogenics*, 26, 1986, 97.
- Tough, J.T. and S.S. Courts, ICEC-12, Southampton, 1988, 312.
- Urbach, A.R., J. Vorreiter and P.V. Mason, ICEC-7, London, 1978, p. 120.
- Urbach, A.R., P.V. Mason and W.F. Brooks, *Adv. Cryog.* 27, 1982, 1039.
- Urbach, A.R. and P.V. Mason, *Adv. Cryog. Eng.* 29, 1984, 651.
- Urban, E.W., L. Katz and G.R. Karr, *Proc. LT-14*, 1985, vol. 4, p.37.
- Urban, E.W. and D.R. Ladner, *Cryogenics* 26, 1986, 122.
- Van Sciver, S.W., et al., *Proc. Space Cryog. Workshop*, Berlin, 1984, p. 37.
- Walstrom, P.L., J.G. Weisend, J.R. Maddocks and S.W. Van Sciver, *Cryogenics* 28, 1988, 101.
- Warren, R.P. et al., ICEC-8, Geneva, 1980, p. 373.
- Weisend, J.G. and S.W. Van Sciver, *Adv. Cryog. Eng.* 33, 1988, 507.
- Yang, L.C., D. Petrac, D.D. Elleman and M.M. Saffren, *Cryog. Proc. & Equipmt.*, ASME Pub. No. H 00164, 1980, p. 141.
- Yeh, T.T. et al., *Cryogenics* 26, 1986, 117.
- Yuan, S.W.K., Ph.D. thesis, UCLA 1985.
- Yuan, S.W.K. and D.J. Frank, *Cryogenics*, 28, 1988, 115.
- Yuan, S.W.K., W.A. Hepler and T.H.K. Frederking, *Proc. 5th Intersoc. Cryog. Sympos.* New Orleans, 1984, p. 169.
- Yuan, S.W.K. and T.H.K. Frederking, *Cryogenics* 27, 1987, 27; *J. Thermophys.* 3, 1989, 406.

Yuan, S.W.K. and T.C. Nast, Adv. Cryog. Eng. 33, 1987, 457.

A P P E N D I X A :

ABSTRACTS OF PAPERS *

This Appendix Section contains either abstracts or extended abstracts of papers related to space cryogenics problems. The work is in part directly related to the NASA grants received , or it is indirectly related to those grants .

*) Additional coauthors have been F. Afifi, P. Abbassi, Bill Chen, W.A. Hepler, P.K. Khandhar, D.Y. Ono .

SLIP EFFECTS ASSOCIATED WITH KNUDSEN TRANSPORT

PHENOMENA IN POROUS MEDIA

Porous media used in phase separators and thermomechanical pumps have been the subject of characterization efforts based on the Darcy permeability of laminar continuum flow (in the "creeping motion" regime). The latter is not always observed at low speed, at particular at permeabilities below 10^{-9} cm^2 . The present experimental and theoretical studies address questions of slip effects associated with long mean free paths of gas flow at room temperature. Data obtained are in good agreement, within data uncertainty, with a simplified asymptotic Knudsen equation proposed for porous plugs on the basis of Knudsen's classical flow equation for long mean free paths.

It is noted that the Knudsen equation has not been used to any significant extent in the literature. (A reason for this may be the symbolics used by Knudsen which departs from today's nomenclature). Knudsen's equation has been derived for tubes and similar ducts not necessarily of circular cross section. Further, Knudsen's equation has an asymptote for moderate ratios of the mean free path (λ) to the characteristic length ($L_c = \lambda^{1/2}$) associated with the system. This asymptote is $\alpha_{\text{eff}} = \alpha (1 + \text{const } \lambda / L_c)$. The present porous media are described, to first order, by

$$\alpha_{\text{eff}} / \alpha = (1 + 1.15 \cdot \lambda / L_c)$$

(sintered stainless steel plugs of phase separators and similar applications).

*) T.H.K. Frederking, W.A. Hepler and P.K. Khandhar, Cryogenics vol. 28, 1988, pp. 110-114.

PERFORMANCE TEST OF A LABORATORY PUMP FOR
LIQUID TRANSFER BASED ON THE FOUNTAIN EFFECT

by

W.E.W.Chen , T.H.K. Frederking and W.A. Hepler

A laboratory scale pump has been tested in detail in order to determine the flow characteristics of a heater-activated all-metal thermomechanical pump (fountain effect pump FEP). The emphasis is on the functional dependence of the fountain pressure difference versus mass throughput. A modified Voté et al. power law approximation is employed for a simplified description of the flow rate as a function of the driving force. Flow rates of up to 10 liters/(hr cm²) have been obtained despite a large nominal pore size of the porous plug of 2 μ m (filtration rating) used for the FEP.

Presented as paper EC-6, CEC/ICMC 87, St. Charles, IL,
June 14-18, 1987.

CRITICAL TRANSPORT PARAMETERS FOR
POROUS MEDIA SUBJECTED TO COUNTERFLOW

T.H.K. Frederking, F.A. Afifi and D.Y. Ono

Experimental and theoretical studies have been conducted to determine critical parameters at the onset of non-linear counterflow in He II below the lambda point of ^4He . Critical temperature differences have been measured in porous media for zero net mass flow and for Darcy permeabilities in the order of magnitude range from 10^{-10} to 10^{-8} cm². The normalized critical temperature gradients, which covered the liquid temperature range of 1.5K to the lambda temperature, are found to vary with T proportional to the ratio of the superfluid density to the normal fluid density. This liquid temperature dependence appears to be consistent with duct data which are limited at low temperature by a Reynolds number criterion.

Keywords: space cryogenics; helium; critical parameters; porous media

Cryogenics vol. 29, 1989, pp. 498-502 ;
Presented at the Space Cryogenics Workshop , Frascati
18-19 July , 1988

ONSET OF VAPORIZATION ASSOCIATED WITH COUNTERFLOW
IN POROUS MEDIA

T.H.K. Frederking, P.K. Khandhar and P. Abbassi

Porous sintered metal plugs have been subjected to counterflow. A step input in power is applied to a heater inside a He I chamber which is connected via the plug to an external He II bath. Phenomena of phase transitions are analyzed on the basis of thermograms obtained: there is liquid He II superheating across the first order phase transition boundary of the vapor pressure curve. Extended vapor domains are produced for high heat inputs when the liquid temperature locally exceeds the homogeneous nucleation temperature.

Proc. ICEC-12; paper C4-5, presented at the ICEC-12 in Southampton, July 12-15, 1988.

S u p p l e m e n t :
Special Invited Sessions at CEC/ICMC'89
on
"1/2 century of superfluid helium"
T.H.K. Frederking, Chairman CEC'89

This "supplement" section presents a few remarks on the "1/2 century.. " sessions at last year's conference at UCLA . Some of these highlights, though considered possibly "historical", pertain significantly to today's discussions on the expanded utilization of He II .

More than 800 participants attended at CEC/ICMC'89. There have been some 500 abstracts, a sizable fraction of which relate to superfluid phenomena including dilution refrigerators. Both space cryogenics liquid management tasks and other He II uses have been of interest. The meeting appears to have been the largest , successful event in the history of the dual conference series. It has been the 8th CEC/ICMC . With the steady increase in scope and volume it is difficult to do justice to all the fine workers and experts in the field. Nevertheless , senior researchers have been asked to give their own impressions, and personal experiences in a field whose accomplishments are considered a common way of life in low temperature technology utilization . The reader is asked not to overlook other papers and authors in the program and

elsewhere.

About half a century has passed since the discovery of the "supereffects" in He II . No clear date appears to be available concerning the actual day of the discovery of a special phase of helium below 2.17 K. Early work in Leiden had already hinted at peculiar phenomena . A milestone achievement appears to have been reached with the 1938/39 publications of the thermomechanical effect, the superfluidity and related observations by Prof. Jack Allen et al., Kapitza and others. At the CEC '89 it has been very gratifying to see the significant and enthusiastic response of authors coming to participate in the "1/2 century.. " sessions. Certainly the 50 years passed gave ample reasons for reflections and thought . Originally only one session had been planned for 1989 however the response indicated more content such that one session addressed lab discoveries while a second one considered He II-applications including large scale systems. - (Due to timing and space constraints , the two sessions could not be accomodated in the logical sequence intended.)

The keynote address in the area was given by plenary speaker Professor W.F. Vinen (paper G-1). Inspecting basic physics, Vinen's presentation raised the provocative question: are there indeed superfluidity applications, such as He II Josephson junctions ? The answer is "no", or better "not yet". Thus, the microscopics has not been

an application item.

In the session (GC) on the early lab discoveries of the He II physics, Professor Jack Allen as most senior pioneer and original discoverer gave a vivid account of what things looked like in those discovery years (GC-1). In particular the use of products of the Allen-Misener technique versus porous plugs appeared to give rise to unexpected results, and switching from one to the other appeared to be on a zig-zag path during the probing of supereffects; (certainly a point appreciated in present day efforts of fountain effect device applications). Dr. William E. Keller , (GC-2), author of one of the early monographs on low temperature helium, emphasized the extensive effort at Los Alamos aiming at a quantification of equilibrium state behavior and transport rates in very narrow slits. This precision work provided a firm basis for various transport regimes described by phenomenological equations. Professor William M. Fairbank (GC-3) has been in most vigorous pursuit of many fundamental physics questions via extensive use and promotion of cryogenics and superconductor technology ; (compare his survey paper at the 1985 MIT CEC/ICMC) . The "Fairbank plug" has been but one of the very useful He II devices. William Fairbank presented lab experiments at Duke and at Stanford University, and his sudden death on Sept. 30, 1989 has been saddening ; (because of his unfinished written version of paper GC-3 no paper documentation will become available). The fact that Bill

Fairbank has come as last minute substitute has been appreciated by this writer in particular. (A rather full account of Bill Fairbank's work is documented in "Near Zero", ed. J.D. Fairbank et al.). Professor Russell J. Donnelly (GC-4) addressed a favorite research topic of his, the quantum vortex and the vortex system. The twisted path toward full appreciation of the role of quantized vortices has led from Onsager and Feynman to many remarkable direct and indirect manifestations of their existence, and fluid dynamics has still to recognize the limit of "high Reynolds number" as a dual case of very high speed and one regime of vortex-free low shear viscosity in combination with rather low speed .

The session (FA) of the "1/2 century" symposium has been devoted to the post-lab discovery part of the work in He II technology areas. Professor Klipping (FA-1) and his group have been pioneering devices for space cryogenics after initial development of novel liquid handling equipment. The focus on superfluid technology development has led to a most challenging and, at the same time, successful path in cryogenic engineering and superconducting magnet stabilization. G. Claudet (FA-2) addressed the latter efforts culminating recently in the large scale TORE SUPRA tokamak system with He II-cooled "D" magnets. Peter Mason (FA-3) has been an eminent space cryogenics pioneer on IRAS along with the coworkers team setting a He II space "milestone". With

this success He II use is continuing in various space projects . Professors N. Nagano and M. Murakami (FA-4 speaker) provided insights into He II cryo- science experiments which appeared to have been conducted not only for basic ideas but also in the context of the Japan technology efforts.

At this occasion a very special "thank you" is conveyed to the invited "1/2 century..."speakers, following the call . Additional acknowledgments go to my colleagues helping along with the 1/2 century symposium. Last , not least , it has been very gratifying to receive written additional input from invited speakers who had been unable to come to CEC/ICMC '89 at the end of July. In reflection on past events J.L. Olsen has looked briefly at the work done at Oxford by the Mendelssohn group , and V. L. Ginzburg has summarized his thoughts on superfluid helium including a possible relationship to "HTSC", the high transition temperature superconductors.

